Research

Contrasting and conserved roles of NPR pathways in diverged land plant lineages

Hyung-Woo Jeon[1]* (iD), Hidekazu Iwakawa[1,2]* (iD), Satoshi Naramoto[3,4] (iD), Cornelia Herrfurth[5,6] (iD), Nora Gutsche[7] (iD), Titus Schlüter[1] (iD), Junko Kyozuka[3] (iD), Shingo Miyauchi[1] (iD), Ivo Feussner[5,6] (iD), Sabine Zachgo[7] (iD) and Hirofumi Nakagami[1] (iD)

[1]Max-Planck Institute for Plant Breeding Research, 50829, Cologne, Germany; [2]School of Biological Science and Technology, College of Science and Engineering, Kanazawa University, Kakuma-machi, Kanazawa, 920-1192, Japan; [3]Graduate School of Life Sciences, Tohoku University, Sendai, 980-8577, Japan; [4]Department of Biological Sciences, Faculty of Science, Hokkaido University, Sapporo, 060-0810, Japan; [5]Service Unit for Metabolomics and Lipidomics, Göttingen Center for Molecular Biosciences (GZMB), University of Göttingen, 37077, Göttingen, Germany; [6]Department for Plant Biochemistry, Albrecht von Haller Institute for Plant Sciences and Göttingen Center for Molecular Biosciences (GZMB), University of Göttingen, 37077, Göttingen, Germany; [7]Division of Botany, Osnabrück University, 49076, Osnabrück, Germany

Author for correspondence:
Hirofumi Nakagami
Email: nakagami@mpipz.mpg.de

Summary

• The NPR proteins function as salicylic acid (SA) receptors in *Arabidopsis thaliana*. AtNPR1 plays a central role in SA-induced transcriptional reprogramming whereby positively regulates SA-mediated defense. NPRs are found in the genomes of nearly all land plants. However, we know little about the molecular functions and physiological roles of NPRs in most plant species.

• We conducted phylogenetic and alignment analyses of NPRs from 68 species covering the significant lineages of land plants. To investigate NPR functions in bryophyte lineages, we generated and characterized NPR loss-of-function mutants in the liverwort *Marchantia polymorpha*.

• Brassicaceae NPR1-like proteins have characteristically gained or lost functional residues identified in AtNPRs, pointing to the possibility of a unique evolutionary trajectory for the Brassicaceae NPR1-like proteins. We find that the only NPR in *M. polymorpha*, MpNPR, is not the master regulator of SA-induced transcriptional reprogramming and negatively regulates bacterial resistance in this species. The Mp*npr* transcriptome suggested roles of MpNPR in heat and far-red light responses. We identify both Mp*npr* and At*npr1-1* display enhanced thermomorphogenesis. Interspecies complementation analysis indicated that the molecular properties of AtNPR1 and MpNPR are partially conserved. We further show that MpNPR has SA-binding activity.

• NPRs and NPR-associated pathways have evolved distinctively in diverged land plant lineages to cope with different terrestrial environments.

Introduction

Land plants deal with various environmental fluctuations or stresses such as shadiness, heat, and drought. Likewise, land plants are constantly surrounded by various microbes and insects and have developed sophisticated immune systems to fight off a wide range of pathogenic organisms. Plant immune responses are controlled by diverse phytohormones such as salicylic acid (SA), jasmonic acid (JA), and ethylene (ET), among which SA has indispensable roles in both local and systemic protection against biotrophic and hemibiotrophic pathogens (Zhou & Zhang, 2020; Peng *et al.*, 2021). In *Arabidopsis thaliana*, NONEXPRESSOR OF PATHOGENESIS-RELATED GENES1 (NPR1) is a central

player in SA-mediated plant immunity. AtNPR1 is responsible for the majority of SA- or benzothiadiazole *S*-methyl ester (BTH; a functional analog of SA)-induced transcriptional reprogramming, positioning AtNPR1 as the master regulator of the regulatory defense network induced by SA in *A. thaliana* (Wang *et al.*, 2006; Blanco *et al.*, 2009). Consistent with this, the controlled expression of AtNPR1 in rice enhances resistance against the bacterial and fungal pathogens, *Xanthomonas oryzae* pv *oryzae*, *Xanthomonas oryzae* pv *oryzicola*, and *Magnaporthe oryzae*, without compromising plant fitness (Xu *et al.*, 2017), underlining the potential of NPR homologs as molecular targets or tools for the engineering of disease-resistant plants.

AtNPR1 contains a Broad-complex, Tramtrack, and Bric-à-brac/poxvirus and zinc finger (BTB/POZ) domain, which interact with repression domain of TGA2 transcription factor; ankyrin

---

*These authors contributed equally to this work.

repeats, which stabilize the NPR1-TGA2 complex; and a C-terminal NPR1-like-C domain, which contains the transactivation domain functioning in NPR1-TGA2 complex (Cao *et al.*, 1997; Ryals *et al.*, 1997; Aravind & Koonin, 1999; Zhang *et al.*, 1999; Li *et al.*, 2006; Rochon *et al.*, 2006; Boyle *et al.*, 2009). The genome of *A. thaliana* encodes four NPR proteins, AtNPR1, AtNPR2, AtNPR3, and AtNPR4. Besides, *A. thaliana* has two BLADE-ON-PETIOLE (BOP) proteins, which are related to NPR proteins (Ha *et al.*, 2004, 2007; Hepworth *et al.*, 2005). Although AtNPR2 is closely related to AtNPR1, the At*npr2* mutant behaves like a wild-type (WT) in response to SA, BTH, and bacterial pathogens (Castelló *et al.*, 2018). However, overexpression of At*NPR2* can partially complement the SA- and BTH-induced resistance phenotype of the At*npr1-1* mutant (Castelló *et al.*, 2018), suggesting functional conservation between AtNPR1 and AtNPR2 as positive regulators of SA signaling. Meanwhile, the At*npr3 npr4* double mutant displays enhanced resistance against bacterial and oomycete pathogens associated with elevated basal pathogen-related (*PR*) gene expression, and AtNPR3 and AtNPR4 have been shown to function as negative regulators of SA signaling (Zhang *et al.*, 2006; Ding *et al.*, 2018).

AtNPR1 to 4 have been demonstrated to function as SA receptors. The SA-binding affinity of AtNPR proteins requires conserved arginine (Arg) residue in the C-terminal NPR1-like-C domains (Fu *et al.*, 2012; Wu *et al.*, 2012; Ding *et al.*, 2018). An AtNPR1 mutant protein with the R432Q substitution failed to bind to SA, and the At*npr1-1* mutant expressing this protein could not complement the SA-insensitivity phenotype (Ding *et al.*, 2018). Similarly, the grass *Brachypodium distachyon* NPR2, BdNPR2 was shown to possess SA-binding ability, which depends on the conserved Arg residue (Shimizu *et al.*, 2022). AtNPR3 and AtNPR4 can function as transcriptional co-repressors, a function conferred by a repression motif, which is related to the ethylene-responsive element binding factor (ERF)-associated amphiphilic repression (EAR) motif (Ohta *et al.*, 2001), found at the C-terminal NPR1-like-C domains of AtNPR3 and AtNPR4 but not AtNPR1 (Ding *et al.*, 2018). Recent structural analysis suggested that SA-binding to AtNPR1 leads to formation of an 'enhanceosome' (Kumar *et al.*, 2022). The structural basis of how AtNPR3 and AtNPR4 function as transcriptional co-repressors remains to be addressed.

AtNPR1 is a cysteine (Cys)-rich protein, and has been proposed to function as a redox sensor (Withers & Dong, 2016). In its inactive state, AtNPR1 forms oligomers through intermolecular disulfide bonds between Cys residues that act to sequester the protein in the cytoplasm (Mou *et al.*, 2003). Importantly, Cys156 of AtNPR1 was shown to be targeted by S-nitrosylation, which facilitates oligomerization (Tada *et al.*, 2008). Intriguingly, a recent study indicated that the disulfide-bridged oligomerization of AtNPR1, which was reported to occur *in vitro*, likely does not occur *in vivo* (Ishihama *et al.*, 2021). Besides, AtNPR1, AtNPR3, and AtNPR4 were shown to regulate protein degradation by recruiting the Cullin 3 E3 ubiquitin ligase, likely through their BTB/POZ domains (Zavaliev *et al.*, 2020).

The monophyletic bryophytes is a sister clade to tracheophytes (Puttick *et al.*, 2018; Leebens-Mack *et al.*, 2019; Li *et al.*, 2020).

The two plant lineages diverged from the common ancestor of the land plants, which evolved from streptophyte algae *c.* 500 million years ago (Bowman *et al.*, 2016; Strother & Taylor, 2018). Such taxonomic importance has placed bryophytes in a significant position in the research of plant evolution and terrestrialization. Bryophytes consist of three divisions: mosses, liverworts, and hornworts (Shaw *et al.*, 2011). The genomes of model bryophytes, the moss *Physcomitrium patens*, the liverwort *Marchantia polymorpha*, and the hornwort *Anthoceros agrestis*, encode two, one, and no NPR homologs, respectively (Bowman *et al.*, 2017; Lang *et al.*, 2018; Li *et al.*, 2020). Notably, expression of *P. patens* Pp*NPR1*/Pp*3c21_7570* can partially restore the *PR1* gene expression and disease resistance phenotypes of the At*npr1-1* mutant, suggesting that the molecular properties of NPR proteins in bryophytes and angiosperms are evolutionarily conserved at some level (Peng *et al.*, 2017). Accumulating evidence shows that ectopic expression of At*NPR1* or NPR homologs in crops, including wheat, tomato, tobacco, and cotton, could alter disease resistance, further supporting functional conservation of NPR proteins in many plant species (Lin *et al.*, 2004; Makandar *et al.*, 2006; Potlakayala *et al.*, 2007; Wally *et al.*, 2009; Parkhi *et al.*, 2010a,b; Gao *et al.*, 2013; Kumar *et al.*, 2013; Matthews *et al.*, 2014; Backer *et al.*, 2019).

Most genetic studies on *NPR* genes that have investigated their physiological roles in different plant species have been carried out in *A. thaliana*. In one rare study in another plant species, in which the authors employed RNAi-based Os*NPR1* knockdown lines in rice, it was reported that Os*NPR1* is responsible for expression levels of 47% of BTH responsive genes (Sugano *et al.*, 2010). However, it is not yet conclusive whether OsNPR1 functions as the master regulator of SA signaling as in *A. thaliana*, because the study was based on knockdown lines, and *Oryza sativa* has two other NPR proteins that may also contribute to SA signaling (Sugano *et al.*, 2010). Therefore, it is still possible that genes other than NPR factors play central roles in SA signaling and that *NPR* genes primarily function in other pathways in plants. In this connection, AtNPR1 was shown to positively regulate cold acclimation in SA- and TGA-independent manners (Olate *et al.*, 2018). Besides, AtNPR1 was described to suppress the unfolded protein response (UPR) independently from SA by interacting with the UPR regulators bZIP28 and bZIP60 (Lai *et al.*, 2018). Here, we address the functional conservation of NPR proteins in plants by utilizing the model liverwort *M. polymorpha* that possesses a single NPR, MpNPR.

Materials and Methods

Plant materials and growth conditions

Marchantia polymorpha accession Tak-1 (Ishizaki *et al.*, 2008) was used as a wild-type throughout this study. For cultivation, gemmae were grown on half-strength Gamborg's B5 (GB5) basal media containing 1% agar at 22°C under continuous white light (60–70 µmol m^{-2} s^{-1}). Sodium salicylate (Sigma-Aldrich) was added to the media for SA-supplemented conditions to achieve desired concentrations. For heat and far-red (FR) light

treatments, gemmae were cultivated in the growth chamber (CLF PlantClimatics, Wertingen, Germany), maintaining continuous white light (400–700 nm, 65 µmol m^{-2} s^{-1}) equipped with FR LEDs (700–780 nm, 65 or 20 µmol m^{-2} s^{-1}) at 22°C or 30°C. Light properties were measured by LI-250A light meter (Li-Cor, Bad Homburg, Germany) equipped with LI-190R quantum sensor (Li-Cor) or SKR110 R/FR sensor (Skye Instruments, Llandrindod Wells, UK).

Arabidopsis thaliana ecotype Col-0 was used as a wild-type in this study. For cultivation of *A. thaliana*, seeds were surface-sterilized by vapor gas (Sodium hypochlorite containing 3% (v/v) HCl) for 4 h and placed on ½-strength Murashige & Skoog media containing 1% agar. Seeds were then incubated at 4°C in the dark for 2 d before germination. Germinated seedlings were cultivated at 22°C under continuous white light (60–70 µmol m^{-2} s^{-1}). For the SA sensitivity test, sodium salicylate (Sigma-Aldrich) was added to the media to achieve desired concentrations.

DNA/RNA extraction and cDNA synthesis

Fresh thalli was ground frozen using a MM 400 mixer mill (Retsch, Haan, Germany). DNA and RNA was extracted using the DNeasy Plant Mini Kit and RNeasy Plant Mini Kit (Qiagen), respectively. cDNA synthesis was performed using SuperScript IV Reverse Transcriptase (Invitrogen).

Plasmid construction and plant transformation

To generate Mp*npr-1^{ge}* and *Mpnpr-2^{ge}* using CRISPR/Cas9 system, the first exon of Mp*NPR* was targeted. The double-strand oligonucleotides containing the target sequences were synthesized and cloned into *pMpGE_En01* or *pMpGE_En03* (Sugano *et al.*, 2018) using In-Fusion HD cloning kit (TaKaRa, Kusatsu, Japan) and *Bsa*I restriction sites in *pMpGE_En03*, respectively. Generated entry clones were subsequently used for the recombination into destination vectors *pMpGE011* and *pMpGE010* (Sugano *et al.*, 2018) by Gateway LR clonase (Thermo Fisher, Waltham, USA) as manufacturer's instruction.

For complementation of *M. polymorpha* Mp*npr* mutants, the full-length CDS of Mp*NPR* (Mp1g02380) and At*NPR1* (At1g64280) were amplified from cDNA of *M. polymorpha* Tak-1 and *A. thaliana* Col-0, respectively. For the MpNPR promoter, 5.6 kb upstream of ATG was amplified from Tak-1 genomic DNA. The amplified fragments were assembled in *pENTR4* (Thermo Fisher) using HiFi assembly master mix (NEB, Ipswich, USA), followed by recombination into *pMpGWB301* (Ishizaki *et al.*, 2015) or *pMpGWB308m* using Gateway LR clonase (Thermo Fisher). For complementation of *A. thaliana* At*npr1-1* mutant, the full-length CDS of Mp*NPR* was amplified from cDNA of *M. polymorpha* ecotype BoGa and cloned into *pBAR-35S* using *Xma*I and *Xba*I restriction sites. The list of primers used in this study are in Supporting Information Table S1.

The resulting constructs were transformed into *Agrobacterium tumefaciens* GV3101, GV2260 or EHA101 by electroporation. Subsequent plant transformations were carried out as described before (Kubota *et al.*, 2013). Obtained transformants were grown on half-strength GB5 basal media containing 1% agar supplemented with 100 µg ml^{-1} cefotaxime and 10 µg ml^{-1} hygromycin B or 0.5 µM chlorsulfuron to screen nonchimeric transgenic gemmae.

Phylogenetic analyses

Amino acid sequences of 317 homologs of MpNPR and AtBOP1 (Table S2) were aligned using CLUSTAL OMEGA with default parameters. To assess the reliability of a phylogenetic tree, the alignment was further calculated using the Maximum Likelihood method with a bootstrap value of 1000 in MEGA (Kumar *et al.*, 2018). For tree visualization and annotation, iTOL was used.

Phytohormones measurements

Marchantia polymorpha thalli were grown on mock and 0.1 mM SA for 14 d before homogenization. Phytohormones were extracted with methyl-tert-butyl ether (MTBE), reversed phase-separated using an ACQUITY UPLC system (Waters Corp, Milford, USA) and analyzed by nanoelectrospray ionization (nanoESI) (TriVersa Nanomate; Advion BioSciences, Ithaca, USA) coupled with an AB Sciex 4000 QTRAP tandem mass spectrometer (AB Sciex, Framingham, USA) employed in scheduled multiple reaction monitoring modes (Herrfurth & Feussner, 2020). For SA measurement, the following mass transition was included 137/93 (declustering potential (DP) −25 V, entrance potential (EP) −6 V, collision energy (CE) −20 V).

Bioluminescence-based bacteria quantification

Bacterial quantification in infected thallus was carried out as described before (Matsumoto *et al.*, 2022). Briefly, *M. polymorpha* were grown on autoclaved cellophane disc on half-strength GB5 media for 2 wk. In the meantime, *Pto-lux* was cultivated in King's B medium containing 30 µg ml^{-1} rifampicin to achieve 1.0 of OD$_{600}$. The saturated bacteria culture was subsequently washed and resuspended in Milli-Q water to prepare bacteria suspension with 0.01 of OD$_{600}$. Next, 2-wk-old thalli were submerged in the bacteria suspension followed by vacuum for 5 min and incubated for 0–3 d on humid filter papers. After incubation, thallus discs (5 mm diameter) were punched from the basal and apical region using a sterile biopsy punch (pfm medical) and transferred to a 96-well plate. The bioluminescence was measured in the FLUOstar Omega plate reader (BMG Labtech, Ortenberg, Germany).

Agrobacterium-mediated transient transformation

Transient transformation was carried out as described before (Iwakawa *et al.*, 2021). A single colony of *A. tumefaciens* strain GV3101::pMP90 harboring $_{pro}$35S:intron-GUSPlus was inoculated into Luria-Bertani medium containing spectinomycin antibiotics and cultured for 2 d at 28°C. Bacterial cells were collected from 1 ml culture by centrifugation, suspended in 5 ml of 0M51C medium (Ono *et al.*, 1979; Takenaka *et al.*, 2000) containing 2% sucrose and 100 µM 3,5-dimethoxy-4-

hydroxyacetophenone (acetosyringone) and cultured for 5 h at 28°C. In parallel, Tak-1 and Mp*npr-1*^{ge} gemmae were cultured on the agar plates for 14 d at 22°C under continuous light. The bacterial culture was diluted with 0M51C medium containing 2% sucrose and 100 μM acetosyringone to be at 0.02 of OD_{600}, and then thalli were transferred into the 50 ml bacterial suspension. The thalli and *Agrobacterium* were co-cultured at 22°C under continuous light for 3 d with shaking (120 rpm).

RNA-Seq and data analyses

Total RNA was isolated from 2-wk-old mature thalli and liquid-grown 7-d-old young gemmae of *M. polymorpha* Tak-1 and Mp*npr-1*^{ge}. For treatments, mature thalli were treated with mock or 1 mM SA for 2, 6, and 12 h, and young gemmae were treated with mock, 1 mM SA, and 0.5 mM BTH for 24 h. Library preparation and sequencing were performed by the Max Planck-Genome-center, Cologne (https://mpgc.mpipz.mpg.de), on the Illumina HiSeq 3000 platform. Raw reads were processed by Fastp (Chen *et al.*, 2018) for quality control and trimming. The *M. polymorpha* genomes and gene annotations (MpTak_v6.1) (Montgomery *et al.*, 2020) were used for mapping reads and counting transcripts per gene using STAR aligner (Dobin *et al.*, 2013). The genes with less than the average of 10 read counts were excluded, and the $\log_2$ fold difference of the gene expression between conditions was calculated by DESEQ2 (Love *et al.*, 2014). Genes with statistical significance (FDR adjusted *P*-value < 0.05) were selected for further analyses.

GUS histochemical assay

Ten-day-old mock- and 0.1 mM SA-grown *A. thaliana* seedlings were submerged in GUS staining solution consisting of 0.5 mg ml^{-1} X-Gluc (5-bromo-4-chloro-3-indolyl-beta-D-glucuronic acid), 0.1% Triton X-100, 10 mM EDTA, 0.5 mM potassium ferricyanide, 0.5 mM potassium ferrocyanide in 100 mM sodium phosphate buffer (pH 7.0), followed by vacuum infiltration for 20 min. After incubation in the dark at 37°C for overnight, leaves were destained by serial incubation in 30%, 50%, 70% ethanol for a minimum of 1 h each before observation.

Recombinant protein preparation and microscale thermophoresis

The AtNPR1, AtNPR1^{R432Q}, MpNPR, and MpNPR^{R413Q} proteins were expressed with N-terminal His^6-MBP tag in BL21 (DE3). Cells were initially grown at 37°C for 2 h and then induced with 0.4 mM isopropyl-β-D-1-thiogalactopyranoside (IPTG) for overnight at 16°C. Cells were harvested and lysed using B-PER complete protein extraction reagent (Thermo Fisher), followed by purification on amylose resin (NEB). Subsequent peak fractions were concentrated to a minimum of 5 μM (Fig. S9b, see later).

His-tag protein labelling and microscale thermophoresis (MST) analysis were performed according to the manufacturer's protocol. Briefly, concentrated proteins were diluted to 500 nM in PBS-T buffer (137 mM NaCl, 2.5 mM KCl, 10 mM Na_2HPO_4, 2 mM KH_2PO_4, pH 7.4, 0.05% Tween-20) and labeled with 100 nM RED-tris-NTA dye (NanoTemper, Munich, Germany) for 30 min at 22°C in the dark. Twenty micromolar sodium salicylate in PBS-T was used for a 1 : 1 serial dilution (16 steps) with a final volume of 10 μl for each step. Subsequently, 10 μl of labeled NPR proteins were added to each step of the dilution series and then incubated for 2 h at 22°C for *in vitro* SA-binding, followed by loading in the Monolith standard capillaries (NanoTemper). Binding affinity assays were performed in the Monolith NT.115 device (NanoTemper) at 22°C with 100% LED and high MST power. The experiment was conducted three times with three independent *in vitro* SA-binding reactions. To calculate the dissociation constant (K_d), data were averaged and fitted in PALMIST (Scheuermann *et al.*, 2016) using the Thermophoresis + T-Jump preset, and then plotted in GUSSI (Brautigam, 2015).

Quantification and statistical analysis

Statistical details, including sample numbers, error bars, and *P*-value cut-offs, were shown in corresponding figure legends. Unless otherwise specified, all statistical significances were calculated in the R using pairwise.t.test with pooled SD. The Benjamini–Hochberg method was then used for correcting the multiple hypothesis testing. Linear regression and calculation of correlation coefficients were performed using the R function lm and cor, respectively.

Results

Brassicaceae NPR1-like proteins possess a peculiar set of functionally important amino acid residues

Extensive studies of AtNPR proteins have identified protein motifs and amino acid residues associated with the molecular mechanisms of how AtNPR proteins induce or repress the expression of SA-responsive genes. To study functional conservation of NPR proteins across different plant species, we performed comprehensive sequence analyses of NPR and BOP homologs. Amino acid sequences of MpNPR (Mp1g02380) and AtBOP1 (At3g57130) were used for BLASTP search against 78 protein databases covering algae, bryophytes, lycophytes, monilophytes, gymnosperms, and angiosperms (Table S3). We identified 194 NPR and 123 BOP homologs in the genomes of 68 species covering the significant lineages of land plants (Table S2). No NPR and BOP homologs were found in streptophyte algae. We found that the exon-intron organization in the regions where the BTB/POZ domains are encoded is highly conserved between NPR and BOP families (Fig. S1). This suggests that NPR and BOP families diverged in the early stage of terrestrialization and may share a common ancestral gene.

Phylogenetic analysis of 194 NPR proteins classified the NPR family into three significant clades; Angiosperms NPR1/2, NPR3/4, and nonseed plants NPR (Fig. 1a). The nonseed plants
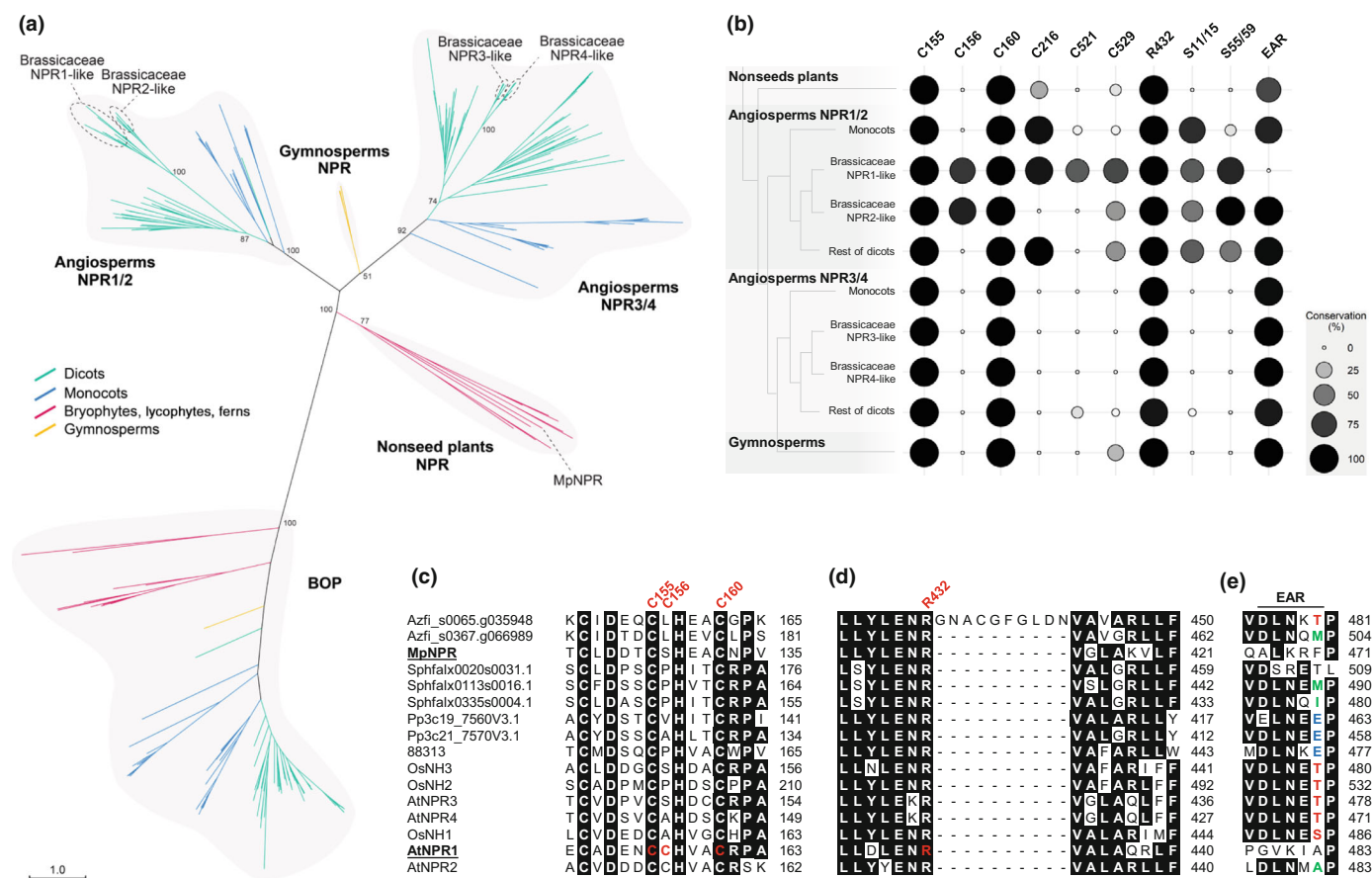
Fig. 1 Phylogenetic analysis and amino acid conservation of 194 NONEXPRESSOR OF PATHOGENESIS-RELATED (NPR) and 123 BLADE-ON-PETIOLE (BOP) proteins from 68 plant species. (a) Unrooted phylogenetic tree showing that 194 NPR proteins were clustered into four major clades; angiosperms NPR1/2, angiosperms NPR3/4, nonseed plants NPR, and gymnosperms NPR clades. Brassicaceae species can be further classified into four subclades: Brassicaceae NPR1-like to Brassicaceae NPR4-like. Numbers indicate bootstrap values. (b–e) Conservation of functional amino acids and motifs associated with the molecular functions of AtNPR1. Cysteines required for AtNPR1 accumulation and oligomerization (c), Arg432 responsible for salicylic acid-binding in AtNPR1 (d), and the EAR motif (DLNxxP) responsible for transcriptional co-repression activity (e) are shown.

clade consists entirely of NPR homologs from bryophytes, lycophytes, and ferns. NPR homologs from angiosperms were clustered into the NPR1/2 and NPR3/4 clades, designated based on AtNPR1/AtNPR2 and AtNPR3/AtNPR4. The phylogenetic tree suggests that angiosperm NPR1/2 and NPR3/4 clades diverged from the ancestral NPR by gene duplication (Fig. 1a). Our comprehensive analysis, including eight Brassicaceae species, revealed that *A. thaliana* gained a further four NPR proteins through additional gene duplication that occurred after the divergence of the Brassicaceae family (Fig. 1a). Consequently, NPR proteins from Brassicaceae species can be further classified into four subclades: Brassicaceae NPR1-like to Brassicaceae NPR4-like (Figs 1a, S2a). Further expansions of *NPR1-like* genes were observed in *Boechera stricta*, *Brassica rapa FPsc*, and *Eutrema salsugineum*, while gene duplication of *NPR2-like*, *NPR3-like*, and *NPR4-like* was not observed except for *NPR3-like* in *B. rapa FPsc* (Fig. S2b). Intriguingly, one of the *B. stricta* NPR1-like proteins, Bostr.29223s0069.1, was found to be integrated into the C-terminus of a Toll/Interleukin-1 receptor/resistance-nucleotide-binding leucine-rich repeat (TIR-NLR) (Fig. S2c),

which implies that Brassicaceae NPR1-like proteins are virulence targets of pathogen effector molecules. In turn, as supported by evidence from *A. thaliana*, Brassicaceae NPR1-like proteins play crucial roles in plant immunity.

We then investigated the conservation of amino acids such as cysteine (Cys), serine (Ser), and arginine (Arg) residues, which are associated with molecular functions of AtNPR1, together with functional motifs including the EAR motif and SUMO interaction motif (SIM) (Figs 1b–e, S3). AtNPR1 forms an oligomer through intermolecular disulfide bonds in its inactive state to reside in the cytoplasm, and several Cys residues were identified to be responsible for the oligomerization or protein accumulation (Mou *et al.*, 2003). For instance, Cys156 is targeted by S-nitrosylation and is required for AtNPR1 oligomerization (Tada *et al.*, 2008; Kumar *et al.*, 2022). Cys521 and Cys529 are critical for transition metal binding activity, and oxidation is required for the SA-dependent co-activation activity of AtNPR1 (Rochon *et al.*, 2006; Wu *et al.*, 2012). We found that Cys155 and Cys160, required for accumulation of AtNPR1 protein (Mou *et al.*, 2003), were conserved in all 194 NPR proteins

(Figs 1b,c, S3). By contrast, Cys156 is conserved only in Brassicaceae NPR1-like and NPR2-like subclades (Figs 1b,c, S3). Cys82 is involved in the oligomerization of AtNPR1 (Mou *et al.*, 2003; Kumar *et al.*, 2022), and we found that Cys82 is well conserved among NPR proteins in all clades and could be detected in 185 out of 194 NPR proteins (Fig. S3). Cys521 and Cys529 are modestly conserved only in Brassicaceae NPR1-like proteins (Figs 1b, S3). Arg432, required for SA-binding in AtNPR1 (Ding *et al.*, 2018), was found to be well conserved among NPR proteins in all clades and was detected in 190 out of 194 NPR proteins (Figs 1b,d, S3). The EAR motif (DLNxxP) of AtNPR3 and AtNPR4 was found to be responsible for their transcriptional co-repressor activities (Ding *et al.*, 2018). Conversely, AtNPR1 was assumed to function as a transcriptional coactivator due to the absence of this motif (Innes, 2018). To our surprise, we found that the EAR motif is conserved in most NPR proteins except for the Brassicaceae NPR1-like proteins (Figs 1b,e, S3). Notably, the EAR motif is well conserved in Brassicaceae NPR2-like, NPR3-like, and NPR4-like proteins (Figs 1b, S3). It is likely that Brassicaceae NPR1-like proteins have lost the EAR motif during evolution. We observed occasional independent losses of the EAR motif in NPR proteins from other plant species, including the single NPR in *M. polymorpha*, MpNPR (Figs 1e, S3). In short, Brassicaceae species have a unique set of NPR proteins, and Brassicaceae NPR1-like proteins may have evolved unique molecular functions as positive regulators of SA-mediated immunity.

NPR negatively regulates the SA response and resistance against bacterial pathogens in *M. polymorpha*

Based on the phylogenetic relationships of NPR proteins and the absence of *NPR* in the genome-sequenced streptophyte algae, functional characterization of NPR proteins from bryophytes would be expected to shed light on the ancestral function of NPR and its evolution. The acquisition of NPR has probably contributed to plant terrestrialization. However, the absence of *NPR* genes in those hornworts for which genomes have been sequenced, namely, *A. agrestis*, *Anthoceros punctatus*, and *Anthoceros angustus*, indicates that NPR is not indispensable for the survival of plants in terrestrial environments. The model liverwort *M. polymorpha* has a single NPR, which is an advantage for efforts aimed at addressing NPR functions. Since AtNPR1 plays a prominent and vital role in SA responses in *A. thaliana*, a comparison of MpNPR and AtNPR1, both of which lack the EAR motif, can contribute to understanding the conservation and diversification of NPR functions. We thus generated CRISPR/Cas9-based NPR loss-of-function mutants in the *M. polymorpha* Tak-1 background. Two guide RNAs were used to target the first exon of Mp*NPR* near the region encoding the BTB/POZ domain and resulted in 26-bp deletion (Mp*npr-1*^{ge}) and 1-bp insertion (Mp*npr-2*^{ge}), respectively (Fig. S4a). Both alleles resulted in a frameshift and early stop codons. We did not observe obvious developmental defects of the Mp*npr* mutants under our growth conditions (Fig. 2a).

Salicylic acid was shown to inhibit the growth of *M. polymorpha*, and thus we first investigated SA and BTH sensitivity of the

Mp*npr* mutants (Gimenez-Ibanez *et al.*, 2019). Tak-1 plants showed no responses in their growth at concentrations up to 0.5 mM SA, while both Mp*npr* mutants displayed growth inhibition only at 0.1 mM SA (Figs 2a,b, S4b,c). Unlike the SA, BTH sensitivity was unchanged in Mp*npr* mutants compared to Tak-1 (Fig. S5). Complemented alleles expressing Mp*NPR* under its own promoter in Mp*npr-1*^{ge} partially rescued the SA hypersensitivity phenotype (Fig. 5a,b, see later; Fig. S4b,c). Moreover, Mp*NPR*-overexpressing plants, $_{pro}$Mp*EF1α*:Mp*NPR-mCitrine*/ Tak-1, displayed reduced sensitivity to the SA treatment (Fig. 5a,b, see later). At*npr1* mutants are characterized by an SA-hypersensitive phenotype due to hyperaccumulation of SA in these mutants (X. Zhang *et al.*, 2010). Therefore, we next measured SA levels in the Mp*npr* mutants to investigate whether the differential SA accumulation contributed to the hypersensitive phenotype. Under our normal growth conditions, SA accumulated to the same levels in the Tak1 and Mp*npr* mutants (Fig. 2c). When plants were grown under SA-supplemented conditions, we observed significantly lower and higher SA levels in Mp*npr-1*^{ge} and Mp*npr-2*^{ge} compared to Tak-1, respectively. However, there was no correlation between the altered SA levels and the growth inhibition phenotype (Fig. 2a–c). In *M. polymorpha*, *dinor*-12-oxo-phytodienoic acid (dn-OPDA) functions as bioactive jasmonate (JA), and antagonism between SA and dn-OPDA was reported (Monte *et al.*, 2018; Gimenez-Ibanez *et al.*, 2019; Matsui *et al.*, 2020). Therefore, we also measured OPDA levels and found that these were not altered in the Mp*npr* mutants (Fig. 2d). Altogether, we concluded that MpNPR negatively regulates SA-dependent growth inhibition.

AtNPR1 positively regulates SA-dependent defense gene expression, and thus At*npr1* mutants display increased susceptibility to various bacterial pathogens (Cao *et al.*, 1997; Roetschi *et al.*, 2001; Backer *et al.*, 2019). Therefore, we investigated whether and how MpNPR contributes to resistance against bacterial pathogens using recently established pathosystems (Iwakawa *et al.*, 2021; Matsumoto *et al.*, 2022). Two-week-old thalli of Tak-1 and Mp*npr* mutants were inoculated with bioluminescent *Pseudomonas syringae* pv *tomato* DC3000 (*Pto*-lux), and bacterial growth was measured at 3 d postinoculation (dpi). *Pto*-lux growth in the Mp*npr* mutants was significantly reduced compared to the growth in Tak-1 in both basal and apical regions of thalli (Fig. 2e). Furthermore, the transient transformation of thalli with *Agrobacterium* carrying *intron-GUSPlus* revealed that Mp*npr-1*^{ge} is more resistant to bacterial infection than Tak-1, shown by less stained air chambers (Fig. 2f,g) (Iwakawa *et al.*, 2021). Note that Mp*npr-1*^{ge} does not change the number of air chambers. These results indicate that MpNPR negatively regulates bacterial resistance in *M. polymorpha*, which implies that MpNPR and AtNPR1 play opposite roles in SA-mediated defense response.

MpNPR is not a master regulator of SA-induced transcriptional reprogramming in *M. polymorpha*

In *A. thaliana*, the vast majority of SA-induced transcriptional reprogramming is governed by AtNPR1, AtNPR3, and AtNPR4 (Wang *et al.*, 2006; Ding *et al.*, 2018). Our results showing that
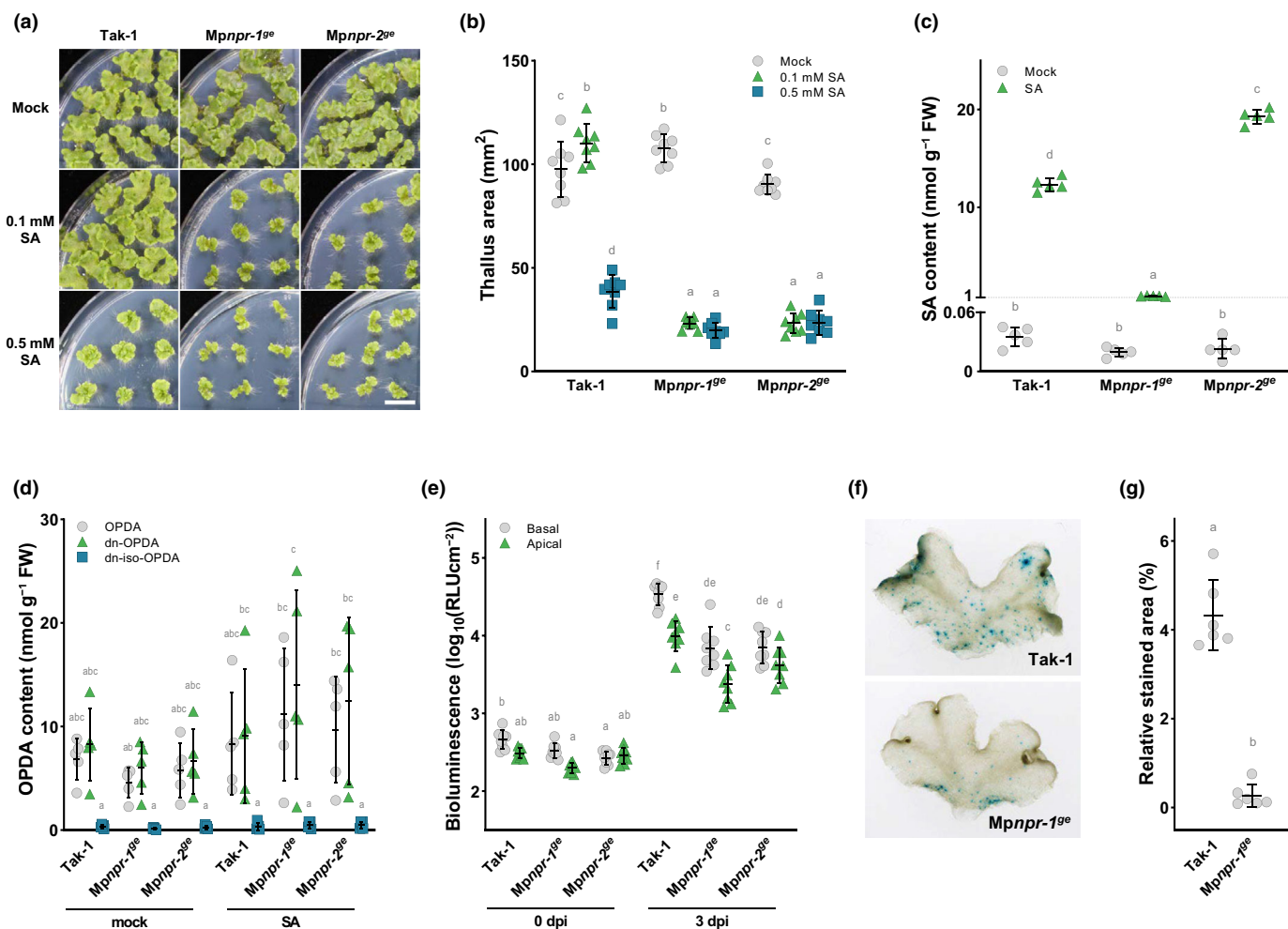
Fig. 2 Phenotypic analyses of Mp*npr* mutants in salicylic acid (SA) and SA-induced immune responses. (a, b) SA hypersensitivity in the growth of Mp*npr-1^{ge}* and Mp*npr-2^{ge}* compared to Tak-1. Bar, 1 cm (n = 8). (c, d) SA and jasmonate measurements in Tak-1 and Mp*npr* mutants grown on mock and SA-supplemented conditions (n = 5). (e) Quantification of bacterial growth in the basal and apical thallus, inoculated with the bioluminescent *Pto*-lux (n = 8). dpi, days postinoculation. (f, g) Transient transformation of Tak-1 and Mp*npr-1^{ge}* using *Agrobacterium* carrying *intron-GUSPlus* (n = 6). (b–e, g) Different letters represent statistical significances (Tukey's test; P < 0.01). Error bars indicate SD.

there is potential for only a single SA receptor in *M. polymorpha*, MpNPR, would suggest that SA-induced transcriptional reprogramming will be lost in the Mp*npr* mutants. To investigate the SA-induced transcriptional response in *M. polymorpha* and the contributions of MpNPR to the response, 2-wk-old Tak-1 and Mp*npr-1^{ge}* plants were treated with 1 mM SA or Mock for 2, 6, and 12 h and subjected to RNA-Seq analysis (Fig. S6a). The number of differentially expressed genes (DEGs, Mock vs SA, |Log$_2$FC| ≥ 1, adjusted P < 0.05) in SA-treated Tak-1 peaked at 6 h postincubation (hpi) (Fig. 3b), and thus we selected a 6 hpi dataset for further analyses. Strikingly, the overall transcriptional response pattern in Mp*npr-1^{ge}* was found to be very similar to the pattern in Tak-1 (Fig. 3a). Similar results were obtained when 7-d-old gemmae, which were grown in a liquid medium, were treated with SA and BTH (Fig. S7). This indicates that the NPR protein is not a master regulator of SA- and BTH-induced transcriptional reprogramming in *M. polymorpha*. Since the transcriptional response was rather pronounced in Mp*npr-1^{ge}*

compared to Tak-1 (Fig. 3b), MpNPR may rather function as a repressor of SA-inducible transcription factors, which is in agreement with the SA hypersensitivity and the bacterial pathogen resistance phenotypes of the Mp*npr* mutants (Fig. 2). Moreover, this implies that other, as yet unknown, molecules likely function as SA receptors in *M. polymorpha*.

In Tak-1, 479 genes were upregulated and 97 genes were downregulated upon SA treatment (Fig. 3b). Gene Ontology (GO) analysis showed significant enrichment of defense-related GO terms, including 'response to wounding' and 'response to other organism', and also GO terms related to responses to various stimuli in up- and downregulated DEGs (Fig. 3c). In Mp*npr-1^{ge}*, 837 genes were upregulated and 887 genes were downregulated upon SA treatment (Fig. 3b). Subsequent GO analysis revealed that GO terms 'response to wounding' is not enriched from the DEGs in Mp*npr-1^{ge}* (Fig. 3d). The expression of some Mp*PR* genes (Carella *et al.*, 2019) was induced by SA treatment, and this upregulation was slightly enhanced in
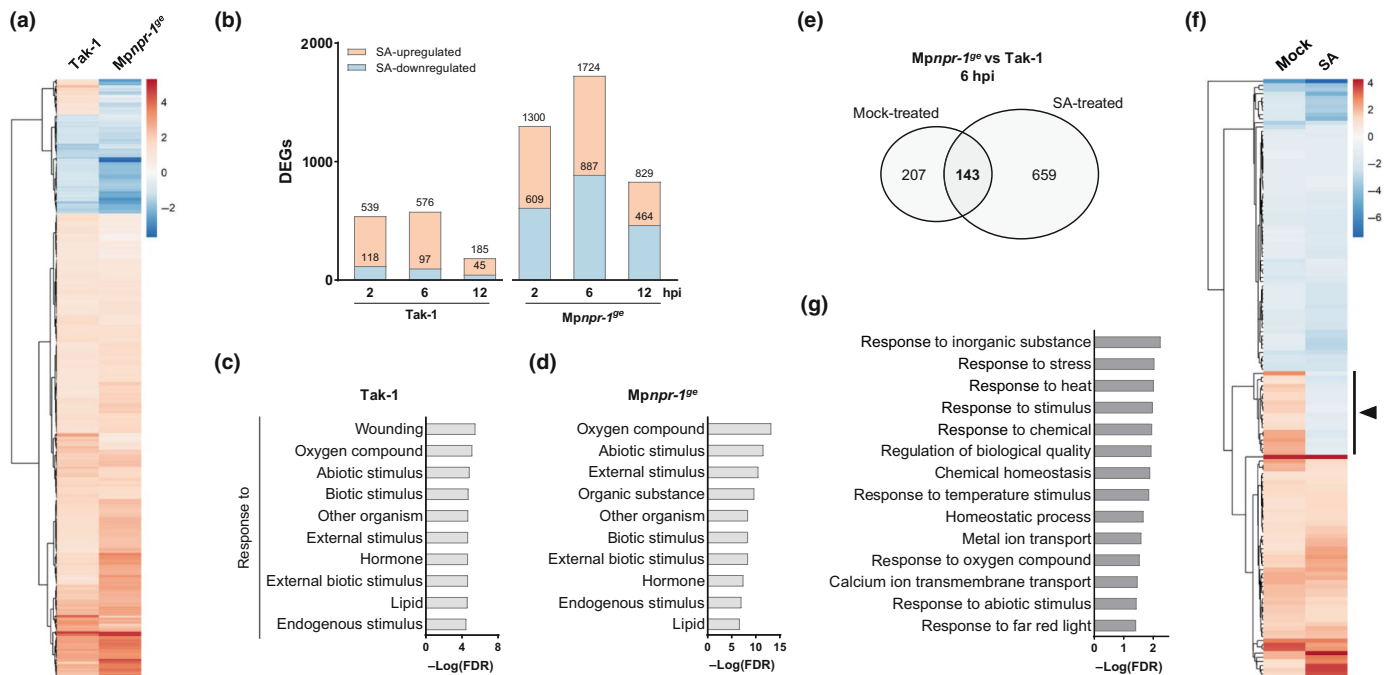
Fig. 3 RNA-Seq analysis comparing salicylic acid (SA)-induced transcriptional reprogramming in Tak-1 and Mp*npr-1^ge*. (a) Heatmap of 425 SA-induced differentially expressed genes (DEGs) ($|log_2FC| \geq 1$, adjusted $P < 0.05$, 6 hpi) identified in Tak-1 and correlated genes in Mp*npr-1^ge*. (b) Number of SA-induced DEGs ($|log_2FC| \geq 1$, adjusted $P < 0.05$) in Tak-1 and Mp*npr-1^ge* for 2, 6, and 12 hpi. (c, d) Gene Ontology (GO) enrichment analyses using SA-induced DEGs (6 hpi) in Tak-1 (c) and Mp*npr-1^ge* (d). Top 10 enrichment of biological process terms beginning with 'response to' are shown (FDR < 0.001). (e) Venn diagram showing numbers of DEGs induced by Mp*npr-1^ge* in each treatment ($|log_2FC| \geq 1$, adjusted $P < 0.05$, 6 hpi). (f) Heatmap of 143 DEGs identified in (e), showing MpNPR-dependent and SA-irresponsive DEGs except for 20 genes (arrowhead). (g) GO enrichment analysis using 123 DEGs identified in (f) (FDR < 0.001). FDR, false discovery rate; hpi, hours postincubation.

Mp*npr-1^ge* compared to Tak-1 (Fig. S6c). These results imply that SA is involved in the defense response and that MpNPR contributes to the SA-dependent wounding-related response.

MpNPR is involved in the heat and far-red light responses

To explore the biological processes that are mediated by NPR but are independent of the SA response in *M. polymorpha*, we compared the transcriptomes of Mp*npr-1^ge* and Tak-1 in response to each treatment. Under Mock- and SA-treated conditions, 350 and 802 genes were identified as DEGs (Mp*npr-1^ge* vs Tak-1, $|Log_2FC| \geq 1$, adjusted $P < 0.05$), respectively (Fig. 3e). Among the DEGs, 143 genes were shared in both Mock- and SA-treated conditions (Fig. 3e,f). In this subset, 20 genes showed significant changes in their expression patterns upon SA treatment (Fig. 3f), and thus, we defined 123 genes as MpNPR-dependent and SA-nonresponsive genes. MpWRKY14 (Mp6g16800) and MpBHLH2 (Mp2g00890) were found in the 20 genes, implying contributions of these transcription factors in MpNPR-dependent SA responses in *M. polymorpha*. Subsequent GO analysis revealed that the biological processes 'response to heat', 'response to temperature stimulus', and 'response to far red light' are over-represented in these 123 genes (Fig. 3g).

To examine whether MpNPR is involved in response to heat, we grew plants at high ambient temperatures, which was previously shown to induce folding and bending of *M. polymorpha*

thalli as a thermomorphogenic response (Ludwig *et al.*, 2021). As reported, enhanced three-dimensional growth of Tak-1 was observed, resulting in upward curling in thallus, when plants were grown at 30°C (Fig. 4a,b). The Mp*npr-1^ge* displayed enhanced curling and bending shown by smaller distance between thallus edge compared to Tak-1 at 30°C (Fig. 4a,b). The Mp*npr-2^ge* showed similar phenotype, but relatively mild, when gemmae were grown 30°C (Fig. S8). Nonetheless, these results indicate that MpNPR negatively regulates thermomorphogenesis in *M. polymorpha*. Then, we asked whether AtNPR1 also plays a role in thermomorphogenesis in *A. thaliana*. Strikingly, we found that the At*npr1-1* mutant and the At*npr1-1 npr3-2 npr4-2* triple mutant display enhanced hypocotyl elongation compared to a wild-type Col-0 and the At*npr3-2 npr4-2* double mutant at 28°C but not at 22°C (Fig. 4c). The *pif4-101* mutant was used as a control (Fig. 4c). These results indicate that both MpNPR and AtNPR1 function as negative regulators of thermomorphogenesis.

We further investigated the possible contribution of MpNPR to far-red (FR) responses in *M. polymorpha*. When Tak-1 was grown in a condition supplemented with FR light, we observed upward thallus growth, similar to shade avoidance responses in angiosperms (Fig. 4d,e) (Casal *et al.*, 1986; Ballaré, 1999; Franklin & Whitelam, 2005). With Mp*PIF* knockout and overexpressing plants as controls, we found that Mp*npr* mutants display reduced upward growth compared to Tak-1 under the FR
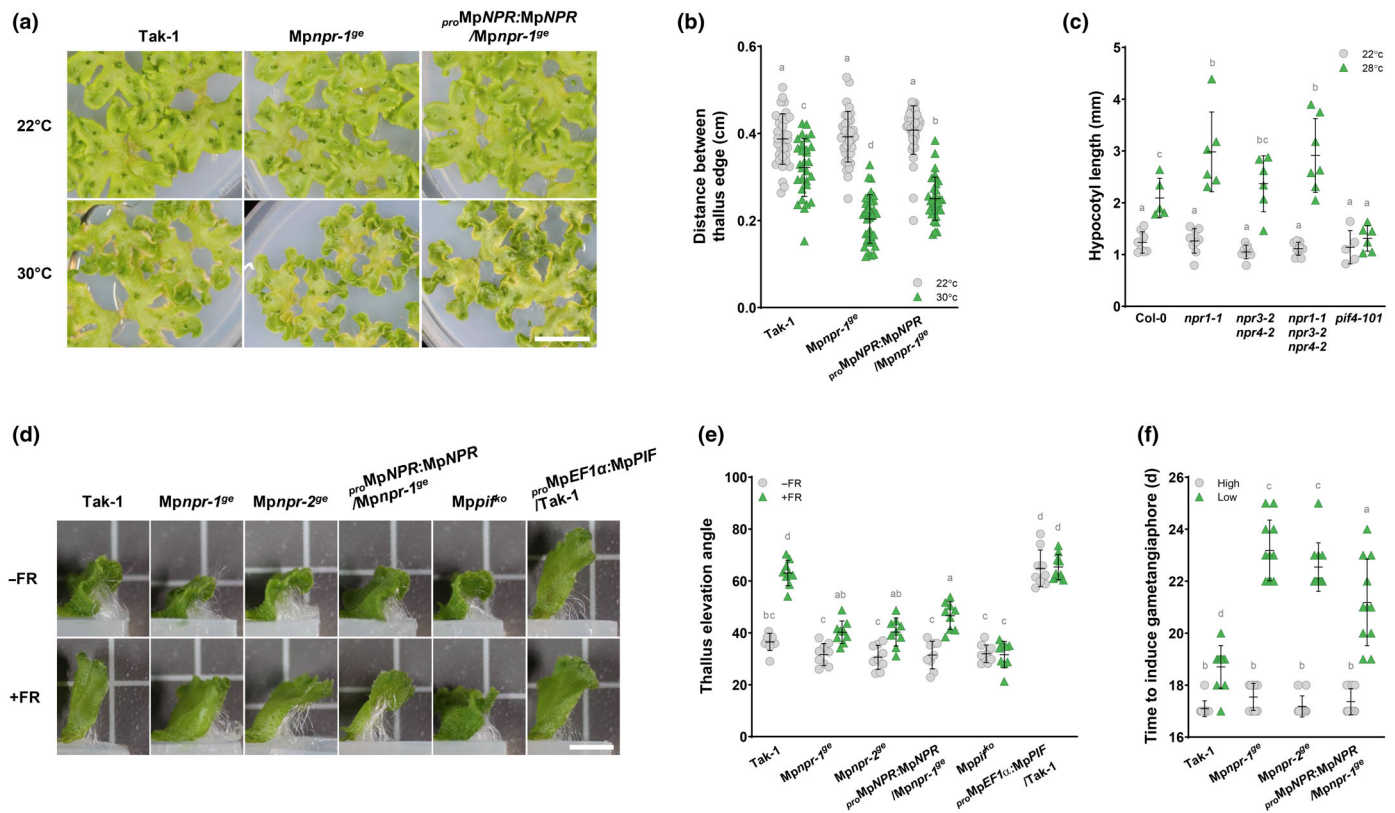
Fig. 4 Putative roles of MpNPR in thermomorphogenesis and shade avoidance syndrome in *Marchantia polymorpha*. (a) Enhanced thermomorphogenesis in the Mp*npr* mutant compared to Tak-1 at 30°C. One-week-old plants were transferred to the indicated conditions and grown for 9 d. Bar, 1 cm. (b) Quantification of altered thermomorphogenesis shown by distance between thallus edges ($n \geq 29$). (c) Hypocotyl length of At*npr* mutants grown at 22°C and 28°C for 6 d ($n \geq 6$). (d) Thallus elevation phenotypes of plants grown with or without far-red light. Bar, 0.5 cm. (e) Quantification of thallus elevation angles from 2-wk-old plants grown with or without far-red light ($n = 9$). (f) Number of days to induce the first gamentangiophore in high and low far-red light (*c*. 65 and 20 µmol m^{-2} s^{-1}, respectively. $n = 11$). (b, c, e, f) Different letters represent statistically significant differences (Tukey's test; $P < 0.01$). Error bars indicate SD.

condition, and the complemented allele displayed a trend toward rescuing the phenotype but was not statistically significant (Fig. 4d,e), which can be due to insufficient expression of MpNPR in this plant compared to Tak-1. Besides, FR-enriched light induces gametangiophore formation in *M. polymorpha*. Under the low red to far-red (R : FR) light condition, Tak-1 and Mp*npr* mutants formed gametangiophore at the same time (Fig. 4f). However, when R : FR ratio was increased, we found that gametangiophore induction was delayed in the Mp*npr* mutants compared to Tak-1, and the complemented allele partially rescued the phenotype (Fig. 4f). These observations support the hypothesis that MpNPR is involved in FR responses in *M. polymorpha*.

Molecular properties are conserved between MpNPR and AtNPR1

Taking an interspecies complementation approach, we next determined whether the molecular properties of NPR proteins from *M. polymorpha* and *A. thaliana* are conserved. Expression of At*NPR1-mCitrine* under the Mp*EF1α* promoter in Mp*npr-1*^{ge} rescued the SA-hypersensitivity phenotype (Fig. 5a,b). Moreover,

*pro*Mp*EF1α:AtNPR1-mCitrine/*Mp*npr-1*^{ge} plants displayed reduced SA sensitivity compared to Tak-1, which is probably due to over-accumulation of AtNPR1 (Fig. 5a,b). Conversely, we expressed MpNPR under the cauliflower mosaic virus (CaMV) 35S promoter in the At*npr1-1* mutant. Expression of Mp*NPR* and At*NPR1* rescued the SA-hypersensitive phenotype (Fig. 5c). Line #4, which failed to express Mp*NPR*, was used as a control (Fig. 5c). The At*npr1-1* mutant possesses the GUS reporter, *BGL2::GUS*, that is responsive to SA accumulation (Cao *et al.*, 1994). In plants treated with SA or BTH, GUS staining was observed only in the complementation lines (Fig. 5d). Taken together, these results indicate that protein functions of MpNPR and AtNPR1 have been conserved to some degree during evolution. Furthermore, these results suggest that NPRs are associated with different components or pathways, which lead to distinct outputs, in different plant species.

MpNPR binds to SA

Given the functional conservation between MpNPR and AtNPR1, we tested the SA-binding activity of MpNPR using MST. Control experiments using His[6]-MBP-AtNPR1 and His[6]-MBP-AtNPR1^{R432Q} showed SA-binding affinity with K_d of
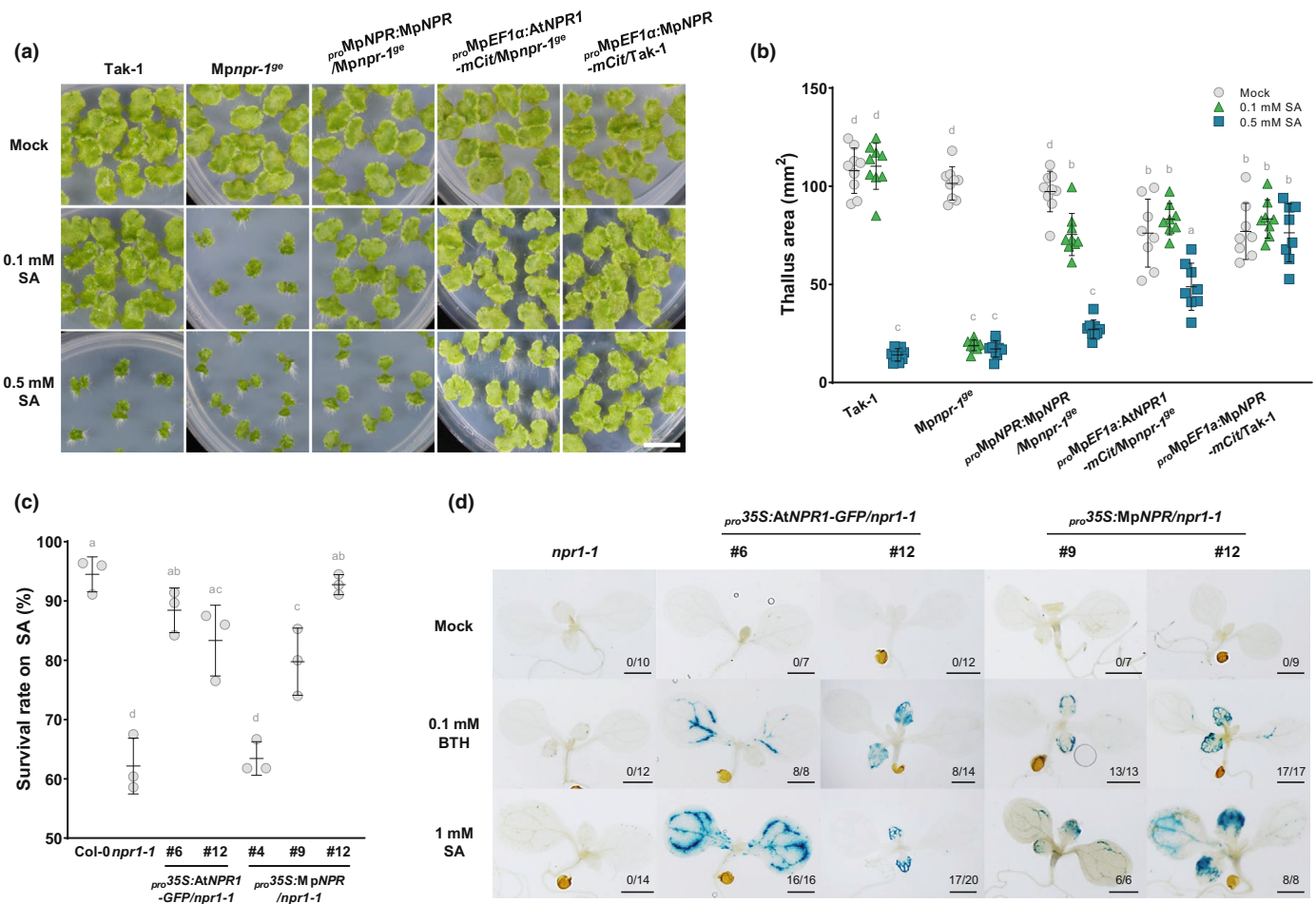
Fig. 5 Interspecies complementation analysis in *Marchantia polymorpha* and *Arabidopsis thaliana*. (a, b) Complementation of salicylic acid (SA) hypersensitivity in Mp*npr-1^ge* by Mp*NPR* and At*NPR1* expression. Bar, 1 cm (*n* = 8). (c) Complementation of SA hypersensitivity in At*npr1-1* by Mp*NPR* and At*NPR1* expression (*n* = 3). (d) GUS staining showed that Mp*NPR* overexpression restored SA- and BTH-induced _pro_*BGL2::GUS* expression in At*npr1-1*. Numbers indicate staining-positive out of all seedling. Bars, 1 mm. (b, c) Different letters represent statistically significant differences (Tukey's test; *P* < 0.01). Error bars indicate SD.

80 ± 40 nM and no binding, respectively, confirming the Arg432-dependent SA-binding of AtNPR1 (Fig. 6a). A dose–response curve using His^6-MBP-MpNPR indicated that MpNPR binds to SA with a K_d of 120 ± 110 nM (Fig. 6a), suggesting that the SA-binding activity is conserved in MpNPR. We also tested whether a change at Arg413 in MpNPR, corresponding to Arg432 in AtNPR1, alters the SA-binding activity of MpNPR. Interestingly, His^6-MBP-MpNPR^{R413Q} still showed the SA-binding activity, but at a reduced level with K_d of 600 ± 400 nM (Fig. 6a). This may indicate that Arg413 of MpNPR is not as critical as Arg432 of AtNPR1, but still functions in SA-binding activity. In agreement with the observation, we found that the expression of Mp*NPR^{R413Q}* could complement the SA-hypersensitivity phenoytpe of Mp*npr-1^ge* (Figs 6b, S9a). Although the SA-binding core (SBC) is highly conserved in MpNPR (Fig. 6c), these results suggest that the SA-binding pocket in MpNPR may have structural differences from those in AtNPRs. Nevertheless, these results suggest that the SA-binding activity is widely conserved in NPR proteins.

Discussion

Our phylogenetic analysis of 194 NPR proteins from 68 land plant species revealed that NPR proteins from angiosperms could be classified into two paralogous clades, NPR1/2 and NPR3/4, presumably diverged from an ancestral NPR (Fig. 1). Two *NPR* genes were found in the genome of *Amborella trichopoda*, the single extant species of the sister lineage to all other angiosperms, and these genes, AmTr_v1.0_scaffold00036.47 and AmTr_v1.0_scaffold00032.72, were classified into the NPR1/2 and NPR3/4 clades, respectively (Table S2). Meanwhile, NPR proteins from gymnosperms formed a single cluster related to neither clade (Fig. 1). This suggests that gene duplication of NPR led to the emergence of the two paralogous clades, seemingly associated with the epsilon whole-genome duplication (WGD) (Albert *et al.*, 2013). Interestingly, the analysis showed that the AtNPR1/AtNPR2 and AtNPR3/AtNPR4 pairs most likely arose from a recent Brassicaceae-specific WGD event (Franzke *et al.*, 2011; Ren *et al.*, 2018), suggesting their functional redundancy in each clade. Indeed, AtNPR3 and AtNPR4
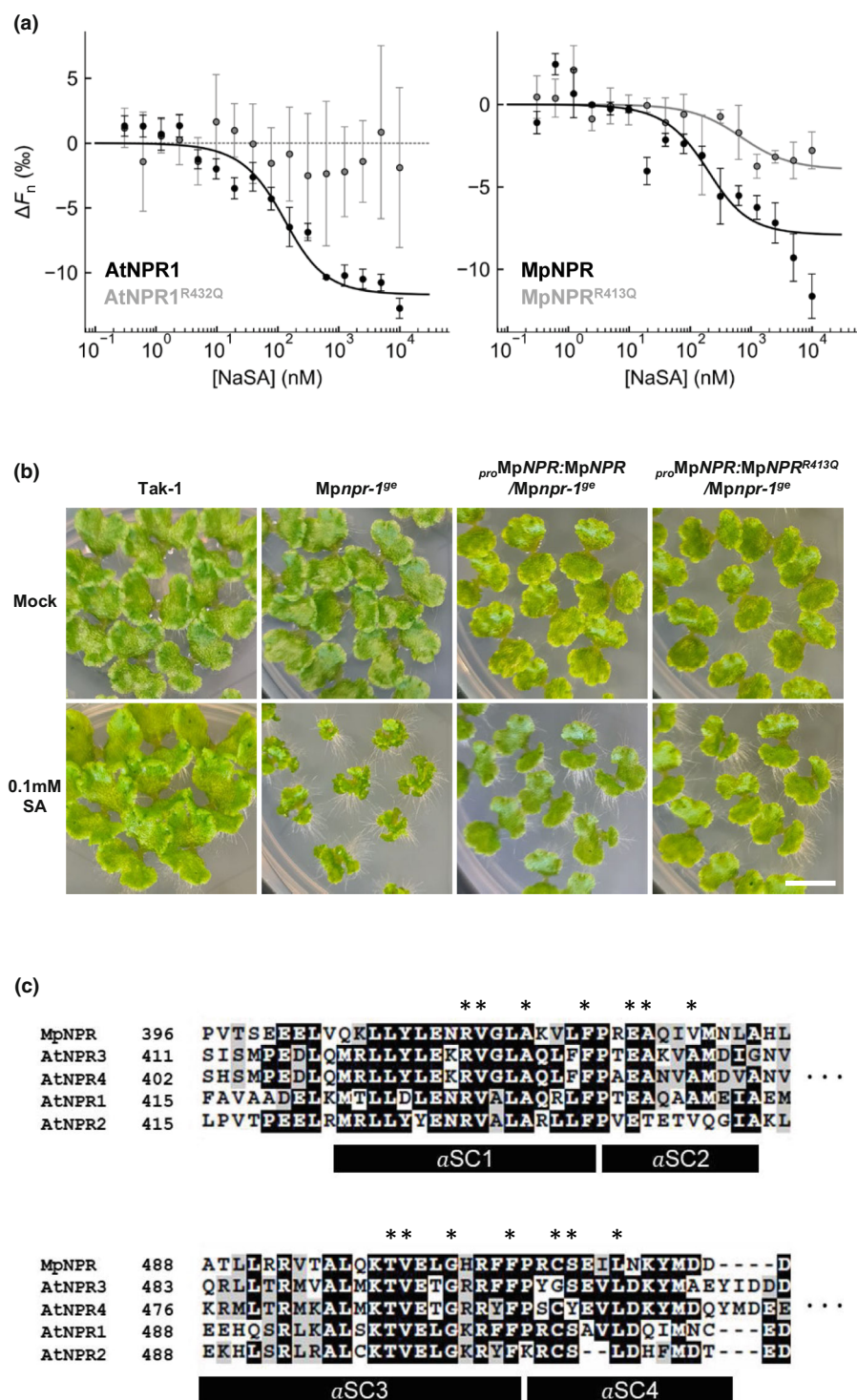
Fig. 6 Salicylic acid (SA)-binding activity of MpNPR. (a) MST affinity analyses of NaSA toward labeled AtNPR1, AtNPR1^{R432Q}, MpNPR, and MpNPR^{R413Q} ($n = 3$, error bars indicate SD). The extracted K_d values were 80 ± 40 nM (AtNPR1), 120 ± 110 nM (MpNPR), and 600 ± 400 nM (MpNPR^{R413Q}). ΔF_n indicates normalized fluorescence. (b) Complementation of SA hypersensitivity in Mp*npr-1^{ge}* by expression of *MpNPR^{R413Q}*. Bar, 1 cm. (c) Conservation of SA-binding core (SBC) in MpNPR and AtNPRs. Four α-helices forming the SA-binding pocket are shown as αSC1 to αSC4 (Wang *et al.*, 2020). Asterisks indicate the core SA-contacting residues.

function redundantly, and AtNPR2, but not AtNPR3 and AtNPR4, can complement At*npr1-1* mutant phenotypes (Zhang *et al.*, 2006; Castelló *et al.*, 2018). Moreover, rice OsNPR1/NH1 and cacao TcNPR1, which belong to the NPR1/2 clade, could complement At*npr1* mutant phenotypes, and overexpression of OsNPR1/NH1 in rice resulted in enhanced resistance against the bacterial pathogen *X. oryzae* pv *oryzae* (Yuan *et al.*, 2007). This suggests functional conservation among NPR proteins in the NPR1/2

clade. Similarly, cacao TcNPR3, which belongs to the NPR3/4 clade, could complement At*npr3-3* mutant phenotypes, and CRISPR/Cas9-based mutagenesis of *TcNPR3* in cacao resulted in enhanced resistance against the cacao pathogen *Phytophthora tropicalis*, suggesting functionally conserved roles for NPR proteins in the NPR3/4 clade as negative regulators of defense responses (Shi *et al.*, 2013; Fister *et al.*, 2018). However, there is a contradictory report, which showed that overexpression of *Nicotiana glutinosa*

NgNPR3, an AtNPR3 homolog, in *Nicotiana tabacum* cv Samsun enhanced resistance to *Alternaria alternata*, *Pseudomonas solanacearum*, and potato virus Y (Y. Zhang *et al.*, 2010). Nevertheless, assuming that NPR proteins from the paralogous clades NPR1/2 and NPR3/4 have acquired opposite or different functions, an obvious question arises of whether and how NPR proteins in the nonseed plants clade, which can be remnants of NPR in the common ancestor of land plants, play roles in SA signaling and defense responses. A single study reported that *P. patens* PpNPR1 partially complements phenotypes of At*npr1-1* but not of At*npr3 npr4* (Peng *et al.*, 2017). Together with our finding that AtNPR1 and MpNPR are interchangeable in the range of evaluated phenotypes, it is likely that the molecular properties of nonseed plant NPR proteins and NPR proteins in NPR1/2 clade have been relatively well conserved during evolution. If so, a remaining question is whether the molecular properties of NPR proteins in the NPR3/4 clade are distinct from nonseed plant NPR proteins. Further genetic studies in many other plant species and interspecies complementation assays will enhance our understanding of the functional conservation and diversification of NPR proteins.

There is compelling evidence that AtNPR1 is the master regulator of SA- or BTH-induced transcriptional reprogramming in *A. thaliana*. However, there is as yet no hint that other Brassicaceae NPR1-like proteins or NPR proteins in the NPR1/2 clade also function as master regulators in their respective species. In order to genetically engineer *NPR* genes to manipulate disease resistance, it is crucial to understand the molecular functions of NPR proteins in other plant species. Further, it remains unclear how AtNPR3 and AtNPR4 have evolved to become transcriptional co-repressors with opposite roles to AtNPR1. One model that has been proposed is that the EAR motif located in the NPR1-like-C domain of AtNPR3 and AtNPR4 differentiates them from AtNPR1, which lacks the EAR motif (Ding *et al.*, 2018). We found that the EAR motif found in AtNPR3 and AtNPR4 is perfectly conserved in all Brassicaceae NPR2-like proteins (Fig. S3), which suggests that Brassicaceae NPR2-like proteins can rather function as transcriptional co-repressors instead of coactivators like AtNPR1. However, as mentioned above, AtNPR2 was shown to complement At*npr1-1* mutant phenotypes. Conservation of the EAR motif in Brassicaceae NPR2-like proteins suggested to us that AtNPR1 or Brassicaceae NPR1-like proteins have presumably lost the EAR motif during evolution. To evaluate this hypothesis, we expanded our analysis of functional protein sequences to all 194 NPR proteins. As expected, we found that the EAR motif is widely conserved in NPR proteins from gymnosperms and all three major clades except for Brassicaceae NPR1-like subclade (Fig. S3). It is formally possible that other NPR proteins have acquired the EAR motif independently during evolution, but we suggest that the more reasonable assumption is that Brassicaceae NPR1-like proteins have lost the EAR motif after a Brassicaceae-specific WGD event. As mentioned above, rice OsNPR1/NH1, cacao TcNPR1, and *P. patens* PpNPR1 could complement phenotypes in At*npr1* mutants (Yuan *et al.*, 2007; Shi *et al.*, 2010; Peng *et al.*, 2017), and these three NPR proteins carry the EAR motif. These observations indicate that the EAR motif is not by itself sufficient for

the co-repressor or coactivator function of NPR proteins. One plausible explanation could be that the EAR motif is controlled by phosphorylation. We found that SP or TP sites in most NPR proteins of dicots in the NPR1/2 clade were substituted with nonphosphorylable hydrophobic residues (A/V/L/I/M) (Fig. S3). Although we have no direct evidence that these sites are targeted by phosphorylation, these clade-specific mutations may further explain how the EAR motif determines protein function.

The remarkable conservation of the Arg residue among NPR proteins, which is required for SA-binding in AtNPR1, AtNPR3, and AtNPR4 (Fu *et al.*, 2012; Wu *et al.*, 2012; Ding *et al.*, 2018), seemingly suggests that NPR proteins generally function as SA receptors in plants. We actually found that MpNPR has SA-binding activity, and the conserved Arg residue contributes to the SA-binding affinity (Fig. 6a). Given that MpNPR was recently shown to act as a MpTGA cofactor in sexual induction (Gutsche *et al.*, 2024), contribution of SA in reproductive processes in liverworts can be investigated. However, unexpected conservation of the EAR motif made it difficult for us to predict how NPR proteins coordinate the SA response in non-Brassicaceae plant species. Rice, *Oryza sativa*, has three NPR proteins, OsNPR1/OsNH1, OsNPR2/OsNH2, and OsNPR3 (Yuan *et al.*, 2007), of which OsNPR1/OsNH1 belongs to the NPR1/2 clade and OsNPR2/OsNH2 and OsNPR3 belong to the NPR3/4 clade (Fig. S3). Overexpression of these three genes in rice suggested that only OsNPR1/OsNH1 functions as a positive regulator of defense responses (Yuan *et al.*, 2007), that is, OsNPR1/OsNH1 but not OsNPR2/OsNH2 or OsNPR3, is a transcriptional coactivator of SA signaling. Accordingly, RNAi-mediated knockdown of Os*NPR1* in rice resulted in impairment of BTH-induced transcriptional reprogramming, but the observed impairment was not as striking as in At*npr1* mutants (Sugano *et al.*, 2010). It is important to generate and analyze Os*npr1* knockout plants, but there is a possibility that release of transcriptional repression by OsNPR2/OsNH2 and OsNPR3 makes a large contribution to the SA response. Analysis of a Os*npr1 npr2 npr3* triple mutant would clarify the contribution of NPR to SA signaling in rice. We found that two NPR proteins in *P. patens* carry the EAR motif but that the single NPR in *M. polymorpha* lacks this motif (Fig. S3). The observation that the expression of MpNPR or PpNPR1 in At*npr1-1* can restore the SA response suggests that bryophyte NPR proteins can function as SA sensing components and transcriptional coactivators in *A. thaliana*, irrespective of the conservation of EAR motif.

It is striking that mutation of the single *NPR* gene in *M. polymorpha*, Mp*NPR*, did not result in diminished SA-induced transcriptional responses, although MpNPR can function as a transcriptional coactivator in *A. thaliana*. Our transcriptomic analysis suggests that MpNPR may function as a transcriptional co-repressor in *M. polymorpha* (Figs 3, S6c). In a similar fashion, the Mp*npr* mutants displayed enhanced resistance against bacterial pathogens (Fig. 2e–g). This is an interesting observation because it implies that NPR is not important for *M. polymorpha* resistance against biotrophic or hemibiotrophic pathogens. Together with the evidence that hornworts have lost the *NPR* gene (Li *et al.*, 2020), NPR may play a less important role in

disease resistance in bryophytes. We speculate that plants have acquired the *NPR* gene during terrestrialization initially for purposes other than SA-mediated immunity. It would be instructive to investigate the functions of NPR in mosses in the future. Besides, it is important to understand why loss of MpNPR or AtNPR1 leads to distinct phenotypes in each species, even though MpNPR and AtNPR1 are exchangeable at some level. Further identification of components that interact with NPRs would help to understand molecular mechanisms behind these intriguing differences.

Our analyses highlighted that Brassicaceae species have evolved a unique NPR repertoire. Marked changes to amino acid sequence were observed to have accumulated in Brassicaceae NPR1-like proteins (Figs 1b, S3). Although we still do not know how these mutations contribute to the molecular functions and physiological roles of Brassicaceae NPR1-like proteins, this finding is rather surprising considering the importance of AtNPR1 in SA signaling and the immune system in *A. thaliana*. Among four Brassicaceae-specific subclades, further lineage-specific expansion of NPR1 was observed (Fig. S2b). This may suggest that Brassicaceae *NPR1-like* genes are experiencing selective pressures. In this respect, AtNPR1 was shown to be targeted by the *P. syringae* type III effector AvrPtoB and *Phytophthora capsici* effector RxLR48 (Chen *et al.*, 2017; Li *et al.*, 2019), further confirming the significance of AtNPR1 in immunity in *A. thaliana*. Effector targets are occasionally integrated into NLR proteins as decoys to counteract pathogen infection (Sarris *et al.*, 2016). Strikingly, we found that one of the *B. stricta* NPR1 homologs, Bostr.29223s0069.1, is integrated into the C-terminus of TIR-NLR (Fig. S2c). Interestingly, BLASTP comparison of this TIR-NLR against the *A. thaliana* database returned SNC1 (suppressor of *npr1-1*, constitutive 1) as a best hit (Zhang *et al.*, 2003). The expression of the TIR-NLR-NPR as a full-length protein needs to be confirmed, but this information seemingly suggests that Brassicaceae NPR1-like proteins generally play a key role in SA-mediated immunity in Brassicaceae species.

What then might have been the ancestral functions of NPR or NPR-associated pathways in the common ancestor of land plants? Our transcriptomic analysis suggested potential roles of MpNPR in heat and FR signaling in *M. polymorpha*. We indeed found that the Mp*npr* mutants display enhanced thermomorphogenesis, reduced FR-induced shade avoidance, and delayed FR-induced gametangiophore formation that was also observed in BoGa Mp*npr* mutants (Fig. 4a,c–e) (Gutsche *et al.*, 2024). Importantly, we revealed that At*npr1-1* also displays enhanced thermomorphogenesis (Fig. 4b), implying that a function of NPR in thermomorphogenesis is conserved in the only two sister lineages of land plants, bryophytes and tracheophytes, and is thus ancient. At*npr1-1* was also reported to display reduced shade avoidance (Nozue *et al.*, 2018). Considering that adaptation to fluctuating temperatures was crucial for plant terrestrialization, it is attractive to hypothesize that plants initially acquired *NPR* genes to deal with varying abiotic components, including temperature and light quality, rather than potentially detrimental microbes. In comparison with the NPR family, the BOP family seems to have undergone less expansion during land plant

evolution. The genome of *A. trichopoda* encodes a single *BOP* gene (Albert *et al.*, 2013), suggesting that *BOP* was not duplicated at the epsilon WGD event. In this regard, the two BOP proteins encoded in the *A. thaliana* genome function redundantly (Hepworth *et al.*, 2005; Norberg *et al.*, 2005; Xu *et al.*, 2010). Nevertheless, analyzed plant species encode between zero and five copies of BOP, suggesting lineage-specific expansion and loss of BOP. The function of *BOP* genes in bryophytes is not yet known, and disruption of all three *BOP* genes in the moss *P. patens* did not cause any observable developmental phenotypes (Hata *et al.*, 2019). It is intriguing that *Marchantia* liverworts have kept the *NPR* gene but lost the *BOP* gene, while *Anthoceros* hornworts have lost the *NPR* gene but kept the *BOP* gene (Bowman *et al.*, 2017; Li *et al.*, 2020). This may imply that *BOP* and *NPR* genes have shared functions that were required for the survival of liverwort and hornwort lineages during evolution. In *A. thaliana*, two BOPs have been shown to play a role in thermomorphogenesis (Zhang *et al.*, 2017), suggesting that AtNPR1 and AtBOP1/2 have shared functions in thermomorphogenesis. Functional analysis of *BOP* genes in hornworts and sophisticated interspecies and intraspecies complementation analysis would shed light on the ancestral shared functions of NPR and BOP proteins or of a hypothetical ancestral protein that diverged into NPR and BOP.

Competing interests

None declared.

Author contributions

H-WJ, HI and HN designed the research. HI performed phylogenetic and alignment analysis. HI, SN and JK generated Mp*npr* mutants. H-WJ and HI generated Mp*npr-1*^{ge} complementation and MpNPR overexpression lines. NG and SZ generated At*npr1-1* complementation lines. H-WJ and HI performed SA and

BTH sensitivity assays. CH and IF quantified phytohormones. H-WJ and TS performed bioluminescence-based bacteria quantification. HI performed transient transformation assay. H-WJ, HI and SM performed transcriptomic analyses. H-WJ performed all other experiments. H-WJ, HI and HN wrote the manuscript. All authors corrected the manuscript. H-WJ and HI contributed equally to this work.

ORCID

Ivo Feussner https://orcid.org/0000-0002-9888-7003
Nora Gutsche https://orcid.org/0000-0002-8306-3087
Cornelia Herrfurth https://orcid.org/0000-0001-8255-3255
Hidekazu Iwakawa https://orcid.org/0000-0002-3362-9978
Hyung-Woo Jeon https://orcid.org/0000-0001-7587-6689
Junko Kyozuka https://orcid.org/0000-0003-2242-7171
Shingo Miyauchi https://orcid.org/0000-0002-0620-5547
Hirofumi Nakagami https://orcid.org/0000-0003-2569-7062
Satoshi Naramoto https://orcid.org/0000-0002-3373-6343
Titus Schlüter https://orcid.org/0000-0001-8281-0565
Sabine Zachgo https://orcid.org/0000-0002-6666-1499

Data availability

References

Albert VA, Barbazuk WB, DePamphilis CW, Der JP, Leebens-Mack J, Ma H, Palmer JD, Rounsley S, Sankoff D, Schuster SC *et al.* **2013.** The *Amborella* genome and the evolution of flowering plants. *Science* **342**: 1241089.

Aravind L, Koonin EV. 1999. Fold prediction and evolutionary analysis of the POZ domain: structural and evolutionary relationship with the potassium channel tetramerization domain. *Journal of Molecular Biology* **285**: 1353–1361.

Backer R, Naidoo S, van den Berg N. 2019. The NONEXPRESSOR OF PATHOGENESIS-RELATED GENES 1 (NPR1) and related family: mechanistic insights in plant disease resistance. *Frontiers in Plant Science* **10**: 1–21.

Ballaré CL. 1999. Keeping up with the neighbours: phytochrome sensing and other signalling mechanisms. *Trends in Plant Science* **4**: 97–102.

Blanco F, Salinas P, Cecchini NM, Jordana X, Van Hummelen P, Alvarez ME, Holuigue L. 2009. Early genomic responses to salicylic acid in Arabidopsis. *Plant Molecular Biology* **70**: 79–102.

Bowman JL, Araki T, Kohchi T. 2016. Marchantia: past, present and future. *Plant and Cell Physiology* **57**: 205–209.

Bowman JL, Kohchi T, Yamato KT, Jenkins J, Shu S, Ishizaki K, Yamaoka S, Nishihama R, Nakamura Y, Berger F *et al.* **2017.** Insights into land plant evolution garnered from the *Marchantia polymorpha* genome. *Cell* **171**: 287–304.

Boyle P, Le Su E, Rochon A, Shearer HL, Murmu J, Chu JY, Fobert PR, Després C. 2009. The BTB/POZ domain of the Arabidopsis disease resistance protein NPR1 interacts with the repression domain of TGA2 to negate its function. *Plant Cell* **21**: 3700–3713.

Brautigam CA. 2015. Calculations and publication-quality illustrations for analytical ultracentrifugation data. *Methods in Enzymology* **562**: 109–133.

Cao H, Bowling SA, Gordon AS, Dong X. 1994. Characterization of an *Arabidopsis* mutant that is nonresponsive to inducers of systemic acquired resistance. *Plant Cell* **6**: 1583.

Cao H, Glazebrook J, Clarke JD, Volko S, Dong X. 1997. The Arabidopsis NPR1 gene that controls systemic acquired resistance encodes a novel protein containing ankyrin repeats. *Cell* **88**: 57–63.

Carella P, Gogleva A, Hoey DJ, Bridgen AJ, Stolze SC, Nakagami H, Schornack S. 2019. Conserved biochemical defenses underpin host responses to oomycete infection in an early-divergent land plant lineage. *Current Biology* **29**: 2282–2294.

Casal JJ, Sanchez RA, Deregibus VA. 1986. The effect of plant density on tillering: the involvement of R/FR ratio and the proportion of radiation intercepted per plant. *Environmental and Experimental Botany* **26**: 365–371.

Castelló MJ, Medina-Puche L, Lamilla J, Tornero P. 2018. NPR1 paralogs of Arabidopsis and their role in salicylic acid perception. *PLoS ONE* **13**: 1–20.

Chen H, Chen J, Li M, Chang M, Xu K, Shang Z, Zhao Y, Palmer I, Zhang Y, McGill J *et al.* **2017.** A bacterial type III effector targets the master regulator of salicylic acid signaling, NPR1, to subvert plant immunity. *Cell Host & Microbe* **22**: 777–788.

Chen S, Zhou Y, Chen Y, Gu J. 2018. FASTP: an ultra-fast all-in-one FASTQ preprocessor. *Bioinformatics* **34**: i884–i890.

Ding Y, Sun T, Ao K, Peng Y, Zhang Y, Li X, Zhang Y. 2018. Opposite roles of salicylic acid receptors NPR1 and NPR3/NPR4 in transcriptional regulation of plant immunity. *Cell* **173**: 1454–1467.

Dobin A, Davis CA, Schlesinger F, Drenkow J, Zaleski C, Jha S, Batut P, Chaisson M, Gingeras TR. 2013. STAR: ultrafast universal RNA-seq aligner. *Bioinformatics* **29**: 15–21.

Fister AS, Landherr L, Maximova SN, Guiltinan MJ. 2018. Transient expression of CRISPR/Cas9 machinery targeting TcNPR3 enhances defense response in *Theobroma cacao*. *Frontiers in Plant Science* **9**: 1–15.

Franklin KA, Whitelam GC. 2005. Phytochromes and shade-avoidance responses in plants. *Annals of Botany* **96**: 169–175.

Franzke A, Lysak MA, Al-Shehbaz IA, Koch MA, Mummenhoff K. 2011. Cabbage family affairs: the evolutionary history of Brassicaceae. *Trends in Plant Science* **16**: 108–116.

Fu ZQ, Yan S, Saleh A, Wang W, Ruble J, Oka N, Mohan R, Spoel SH, Tada Y, Zheng N *et al.* **2012.** NPR3 and NPR4 are receptors for the immune signal salicylic acid in plants. *Nature* **486**: 228–232.

Gao CS, Kou XJ, Li HP, Zhang JB, Saad ASI, Liao YC. 2013. Inverse effects of Arabidopsis NPR1 gene on *Fusarium* seedling blight and *Fusarium* head blight in transgenic wheat. *Plant Pathology* **62**: 383–392.

Gimenez-Ibanez S, Zamarreño AM, García-Mina JM, Solano R. 2019. An evolutionarily ancient immune system governs the interactions between *Pseudomonas syringae* and an early-diverging land plant lineage. *Current Biology* **29**: 2270–2281.

Gutsche N, Koczula J, Trupp M, Holtmannspötter M, Appelfeller M, Rupp O, Busch A, Zachgo S. 2024. MpTGA, together with MpNPR, regulates sexual reproduction and independently affects oil body formation in *Marchantia polymorpha*. *New Phytologist* **241**: 1559–1573.

Ha CM, Ji HJ, Hong GN, Fletcher JC. 2007. BLADE-ON-PETIOLE1 and 2 control Arabidopsis lateral organ fate through regulation of LOB domain and adaxial-abaxial polarity genes. *Plant Cell* **19**: 1809–1825.

Ha CM, Jun JH, Nam HG, Fletcher JC. 2004. BLADE-ON-PETIOLE1 encodes a BTB/POZ domain protein required for leaf morphogenesis in *Arabidopsis thaliana*. *Plant and Cell Physiology* **45**: 1361–1370.

Hata Y, Naramoto S, Kyozuka J. 2019. BLADE-ON-PETIOLE genes are not involved in the transition from protonema to gametophore in the moss *Physcomitrella patens*. *Journal of Plant Research* **132**: 617–627.

Hepworth SR, Zhang Y, McKim S, Li X, Haughn GW. 2005. BLADE-ON-PETIOLE–dependent signaling controls leaf and floral patterning in Arabidopsis. *Plant Cell* **17**: 1434–1448.

Herrfurth C, Feussner I. 2020. Quantitative jasmonate profiling using a high-throughput UPLC-NanoESI-MS/MS method. In: Champion A, Laplaze L, eds. *Jasmonate in plant biology, methods in molecular biololgy*. New York, NY, USA: Humana, 169–187.

Innes R. 2018. The positives and negatives of NPR: a unifying model for salicylic acid signaling in plants. *Cell* **173**: 1314–1315.

Ishihama N, Choi S, Noutoshi Y, Saska I, Asai S, Takizawa K, He SY, Osada H, Shirasu K, Takizawa K. 2021. Oxicam-type non-steroidal anti-inflammatory

drugs inhibit NPR1-mediated salicylic acid pathway. *Nature Communications* **12**: 7303.

Ishizaki K, Chiyoda S, Yamato KT, Kohchi T. 2008. *Agrobacterium*-mediated transformation of the haploid liverwort *Marchantia polymorpha* L., an emerging model for plant biology. *Plant and Cell Physiology* **49**: 1084–1091.

Ishizaki K, Nishihama R, Ueda M, Inoue K, Ishida S, Nishimura Y, Shikanai T, Kohchi T. 2015. Development of gateway binary vector series with four different selection markers for the liverwort *Marchantia polymorpha*. *PLoS ONE* **10**: e0138876.

Iwakawa H, Melkonian K, Schlüter T, Jeon H-W, Nishihama R, Motose H, Nakagami H. 2021. *Agrobacterium*-mediated transient transformation of *Marchantia* liverworts. *Plant and Cell Physiology* **62**: 1718–1727.

Kubota A, Ishizaki K, Hosaka M, Kohchi T. 2013. Efficient *Agrobacterium*-mediated transformation of the liverwort *Marchantia polymorpha* using regenerating thalli. *Bioscience, Biotechnology, and Biochemistry* **77**: 167–172.

Kumar S, Stecher G, Li M, Knyaz C, Tamura K. 2018. MEGA X: molecular evolutionary genetics analysis across computing platforms. *Molecular Biology and Evolution* **35**: 1547–1549.

Kumar S, Zavaliev R, Wu Q, Zhou Y, Cheng J, Dillard L, Powers J, Withers J, Zhao J, Guan Z et al. 2022. Structural basis of NPR1 in activating plant immunity. *Nature* **605**: 561–566.

Kumar V, Joshi SG, Bell AA, Rathore KS. 2013. Enhanced resistance against *Thielaviopsis basicola* in transgenic cotton plants expressing Arabidopsis NPR1 gene. *Transgenic Research* **22**: 359–368.

Lai Y-S, Renna L, Yarema J, Ruberti C, He SY, Brandizzi F. 2018. Salicylic acid-independent role of NPR1 is required for protection from proteotoxic stress in the plant endoplasmic reticulum. *Proceedings of the National Academy of Sciences, USA* **115**: E5203–E5212.

Lang D, Ullrich KK, Murat F, Fuchs J, Jenkins J, Haas FB, Piednoel M, Gundlach H, Van Bel M, Meyberg R et al. 2018. The *Physcomitrella patens* chromosome-scale assembly reveals moss genome structure and evolution. *The Plant Journal* **93**: 515–533.

Leebens-Mack JH, Barker MS, Carpenter EJ, Deyholos MK, Gitzendanner MA, Graham SW, Grosse I, Li Z, Melkonian M, Mirarab S et al. 2019. One thousand plant transcriptomes and the phylogenomics of green plants. *Nature* **574**: 679–685.

Li F-W, Nishiyama T, Waller M, Frangedakis E, Keller J, Li Z, Fernandez-Pozo N, Barker MS, Bennett T, Blázquez MA et al. 2020. Anthoceros genomes illuminate the origin of land plants and the unique biology of hornworts. *Nature Plants* **6**: 259–272.

Li J, Mahajan A, Tsai M-D. 2006. Ankyrin repeat: a unique motif mediating protein−protein interactions. *Biochemistry* **45**: 15168–15178.

Li Q, Chen Y, Wang J, Zou F, Jia Y, Shen D, Zhang Q, Jing M, Dou D, Zhang M. 2019. A *Phytophthora capsici* virulence effector associates with NPR1 and suppresses plant immune responses. *Phytopathology Research* **1**: 6.

Lin W-C, Lu C-F, Wu J-W, Cheng M-L, Lin Y-M, Yang N-S, Black L, Green SK, Wang J-F, Cheng C-P. 2004. Transgenic tomato plants expressing the Arabidopsis NPR1 gene display enhanced resistance to a spectrum of fungal and bacterial diseases. *Transgenic Research* **13**: 567–581.

Love MI, Huber W, Anders S. 2014. Moderated estimation of fold change and dispersion for RNA-seq data with DESeq2. *Genome Biology* **15**: 1–21.

Ludwig W, Hayes S, Trenner J, Delker C, Quint M. 2021. On the evolution of plant thermomorphogenesis. *Journal of Experimental Botany* **72**: 7345–7358.

Makandar R, Essig JS, Schapaugh MA, Trick HN, Shah J. 2006. Genetically engineered resistance to *Fusarium* head blight in wheat by expression of Arabidopsis NPR1. *Molecular Plant–Microbe Interactions* **19**: 123–129.

Matsui H, Iwakawa H, Hyon G-S, Yotsui I, Katou S, Monte I, Nishihama R, Franzen R, Solano R, Nakagami H. 2020. Isolation of natural fungal pathogens from *Marchantia polymorpha* reveals antagonism between salicylic acid and jasmonate during liverwort–fungus interactions. *Plant and Cell Physiology* **61**: 265–275.

Matsumoto A, Schlüter T, Melkonian K, Takeda A, Nakagami H, Mine A. 2022. A versatile Tn7 transposon-based bioluminescence tagging tool for quantitative and spatial detection of bacteria in plants. *Plant Communications* **3**: 100227.

Matthews BF, Beard H, Brewer E, Kabir S, MacDonald MH, Youssef RM. 2014. Arabidopsis genes, AtNPR1, AtTGA2 and AtPR-5, confer partial resistance to soybean cyst nematode (*Heterodera glycines*) when overexpressed in transgenic soybean roots. *BMC Plant Biology* **14**: 96.

Monte I, Ishida S, Zamarreño AM, Hamberg M, Franco-Zorrilla JM, García-Casado G, Gouhier-Darimont C, Reymond P, Takahashi K, García-Mina JM et al. 2018. Ligand-receptor co-evolution shaped the jasmonate pathway in land plants. *Nature Chemical Biology* **14**: 480–488.

Montgomery SA, Tanizawa Y, Galik B, Wang N, Ito T, Mochizuki T, Akimcheva S, Bowman JL, Cognat V, Maréchal-Drouard L et al. 2020. Chromatin organization in early land plants reveals an ancestral association between H3K27me3, transposons, and constitutive heterochromatin. *Current Biology* **30**: 573–588.

Mou Z, Fan W, Dong X. 2003. Inducers of plant systemic acquired resistance regulate NPR1 function through redox changes. *Cell* **113**: 935–944.

Norberg M, Holmlund M, Nilsson O. 2005. The BLADE ON PETIOLE genes act redundantly to control the growth and development of lateral organs. *Development* **132**: 2203–2213.

Nozue K, Devisetty UK, Lekkala S, Mueller-Moulé P, Bak A, Casteel CL, Maloof JN. 2018. Network analysis reveals a role for salicylic acid pathway components in shade avoidance. *Plant Physiology* **178**: 1720–1732.

Ohta M, Matsui K, Hiratsu K, Shinshi H, Ohme-Takagi M. 2001. Repression domains of class II ERF transcriptional repressors share an essential motif for active repression. *Plant Cell* **13**: 1959.

Olate E, Jiménez-Gómez JM, Holuigue L, Salinas J. 2018. NPR1 mediates a novel regulatory pathway in cold acclimation by interacting with HSFA1 factors. *Nature Plants* **4**: 811–823.

Ono K, Ohyama K, Gamborg OL. 1979. Regeneration of the liverwort *Marchantia polymorpha* L. from protoplasts isolated from cell suspension culture. *Plant Science Letters* **14**: 225–229.

Parkhi V, Kumar V, Campbell LAM, Bell AA, Rathore KS, Campbell B, Rathore KS. 2010a. Expression of Arabidopsis NPR1 in transgenic cotton confers resistance to non-defoliating isolates of *Verticillium dahliae* but not the defoliating isolates. *Journal of Phytopathology* **158**: 822–825.

Parkhi V, Kumar V, Campbell LAM, Bell AA, Shah J, Rathore KS. 2010b. Resistance against various fungal pathogens and reniform nematode in transgenic cotton plants expressing Arabidopsis NPR1. *Transgenic Research* **19**: 959–975.

Peng Y, Sun T, Zhang Y. 2017. Perception of salicylic acid in *Physcomitrella patens*. *Frontiers in Plant Science* **8**: 2145.

Peng Y, Yang J, Li X, Zhang Y. 2021. Salicylic acid: biosynthesis and signaling. *Annual Review of Plant Biology* **72**: 761–791.

Potlakayala SD, DeLong C, Sharpe A, Fobert PR. 2007. Conservation of NON-EXPRESSOR OF PATHOGENESIS-RELATED GENES1 function between *Arabidopsis thaliana* and *Brassica napus*. *Physiological and Molecular Plant Pathology* **71**: 174–183.

Puttick MN, Morris JL, Williams TA, Cox CJ, Edwards D, Kenrick P, Pressel S, Wellman CH, Schneider H, Pisani D et al. 2018. The interrelationships of land plants and the nature of the ancestral embryophyte. *Current Biology* **28**: 733–745.

Ren R, Wang H, Guo C, Zhang N, Zeng L, Chen Y, Ma H, Qi J. 2018. Widespread whole genome duplications contribute to genome complexity and species diversity in angiosperms. *Molecular Plant* **11**: 414–428.

Rochon A, Boyle P, Wignes T, Fobert PR, Després C. 2006. The coactivator function of Arabidopsis NPR1 requires the core of its BTB/POZ domain and the oxidation of C-terminal cysteines. *Plant Cell* **18**: 3670–3685.

Roetschi A, Si-Ammour A, Belbahri L, Mauch F, Mauch-Mani B. 2001. Characterization of an *Arabidopsis-Phytophthora* pathosystem: resistance requires a functional PAD2 gene and is independent of salicylic acid, ethylene and jasmonic acid signalling. *The Plant Journal* **28**: 293–305.

Ryals J, Weymann K, Lawton K, Friedrich L, Ellis D, Steiner HY, Johnson J, Delaney TP, Jesse T, Vos P et al. 1997. The Arabidopsis NIM1 protein shows homology to the mammalian transcription factor inhibitor I kappa B. *Plant Cell* **9**: 425–439.

Sarris PF, Cevik V, Dagdas G, Jones JDG, Krasileva KV. 2016. Comparative analysis of plant immune receptor architectures uncovers host proteins likely targeted by pathogens. *BMC Biology* **14**: 8.

Scheuermann TH, Padrick SB, Gardner KH, Brautigam CA. 2016. On the acquisition and analysis of microscale thermophoresis data. *Analytical Biochemistry* **496**: 79–93.

Shaw AJ, Szövényi P, Shaw B. 2011. Bryophyte diversity and evolution: windows into the early evolution of land plants. *American Journal of Botany* **98**: 352–369.

Shi Z, Maximova SN, Liu Y, Verica J, Guiltinan MJ. 2010. Functional analysis of the *Theobroma cacao* NPR1 gene in Arabidopsis. *BMC Plant Biology* **10**: 248.

New
Phytologist

Shi Z, Zhang Y, Maximova SN, Guiltinan MJ. 2013. TcNPR3 from *Theobroma cacao* functions as a repressor of the pathogen defense response. *BMC Plant Biology* 13: 1–12.

Shimizu K, Suzuki H, Uemura T, Nozawa A, Desaki Y, Hoshino R, Yoshida A, Abe H, Nishiyama M, Nishiyama C *et al.* 2022. Immune gene activation by NPR and TGA transcriptional regulators in the model monocot *Brachypodium distachyon*. *The Plant Journal* 110: 470–481.

Strother PK, Taylor WA. 2018. The evolutionary origin of the plant spore in relation to the antithetic origin of the plant sporophyte. In: Krings M, Harper CJ, Cúneo NR, Rothwell GW, eds. *Transformative paleobotany: papers to commemorate the life and legacy of Thomas N. Taylor*. Amsterdam, the Netherlands: Elsevier, 3–20.

Sugano S, Jiang CJ, Miyazawa SI, Masumoto C, Yazawa K, Hayashi N, Shimono M, Nakayama A, Miyao M, Takatsuji H. 2010. Role of OsNPR1 in rice defense program as revealed by genome-wide expression analysis. *Plant Molecular Biology* 74: 549–562.

Sugano SS, Nishihama R, Shirakawa M, Takagi J, Matsuda Y, Ishida S, Shimada T, Hara-Nishimura I, Osakabe K, Kohchi T. 2018. Efficient CRISPR/Cas9-based genome editing and its application to conditional genetic analysis in *Marchantia polymorpha*. *PLoS ONE* 13: e0205117.

Tada Y, Spoel SH, Pajerowska-Mukhtar K, Mou Z, Song J, Wang C, Zuo J, Dong X. 2008. Plant immunity requires conformational charges of NPR1 via S-nitrosylation and thioredoxins. *Science* 321: 952–956.

Takenaka M, Yamaoka S, Hanajiri T, Shimizu-Ueda Y, Yamato KT, Fukuzawa H, Ohyama K. 2000. Direct transformation and plant regeneration of the haploid liverwort *Marchantia polymorpha* L. *Transgenic Research* 9: 179–185.

Wally O, Jayaraj J, Punja ZK. 2009. Broad-spectrum disease resistance to necrotrophic and biotrophic pathogens in transgenic carrots (*Daucus carota* L.) expressing an Arabidopsis NPR1 gene. *Planta* 231: 131–141.

Wang D, Amornsiripanitch N, Dong X. 2006. A genomic approach to identify regulatory nodes in the transcriptional network of systemic acquired resistance in plants. *PLoS Pathogens* 2: e123.

Wang W, Withers J, Li H, Zwack PJ, Rusnac D-V, Shi H, Liu L, Yan S, Hinds TR, Guttman M *et al.* 2020. Structural basis of salicylic acid perception by Arabidopsis NPR proteins. *Nature* 586: 311–316.

Withers J, Dong X. 2016. Posttranslational modifications of NPR1: a single protein playing multiple roles in plant immunity and physiology. *PLoS Pathogens* 12: 1–9.

Wu Y, Zhang D, Chu JY, Boyle P, Wang Y, Brindle ID, De Luca V, Després C. 2012. The Arabidopsis NPR1 protein is a receptor for the plant defense hormone salicylic acid. *Cell Reports* 1: 639–647.

Xu G, Yuan M, Ai C, Liu L, Zhuang E, Karapetyan S, Wang S, Dong X. 2017. UORF-mediated translation allows engineered plant disease resistance without fitness costs. *Nature* 545: 491–494.

Xu M, Hu T, McKim SM, Murmu J, Haughn GW, Hepworth SR. 2010. Arabidopsis BLADE-ON-PETIOLE1 and 2 promote floral meristem fate and determinacy in a previously undefined pathway targeting APETALA1 and AGAMOUS-LIKE24. *The Plant Journal* 63: 974–989.

Yuan Y, Zhong S, Li QQ, Zhu Z, Lou Y, Wang L, Wang J, Wang M, Li QQ, Yang D *et al.* 2007. Functional analysis of rice NPR1-like genes reveals that OsNPR1/NH1 is the rice orthologue conferring disease resistance with enhanced herbivore susceptibility. *Plant Biotechnology Journal* 5: 313–324.

Zavaliev R, Mohan R, Chen T, Dong X. 2020. Formation of NPR1 condensates promotes cell survival during the plant immune response. *Cell* 119: 1–16.

Zhang B, Holmlund M, Lorrain S, Norberg M, Bakó LS, Fankhauser C, Nilsson O. 2017. BLADE-ON-PETIOLE proteins act in an E3 ubiquitin ligase complex to regulate PHYTOCHROME INTERACTING FACTOR 4 abundance. *eLife* 6: 1–19.

Zhang X, Chen S, Mou Z. 2010. Nuclear localization of NPR1 is required for regulation of salicylate tolerance, isochorismate synthase 1 expression and salicylate accumulation in *Arabidopsis*. *Journal of Plant Physiology* 167: 144–148.

Zhang Y, Cheng YT, Qu N, Zhao Q, Bi D, Li X. 2006. Negative regulation of defense responses in Arabidopsis by two NPR1 paralogs. *The Plant Journal* 48: 647–656.

Zhang Y, Fan W, Kinkema M, Li X, Dong X. 1999. Interaction of NPR1 with basic leucine zipper protein transcription factors that bind sequences required for salicylic acid induction of the PR-1 gene. *Proceedings of the National Academy of Sciences, USA* 96: 6523–6528.

Zhang Y, Goritschnig S, Dong X, Li X. 2003. A gain-of-function mutation in a plant disease resistance gene leads to constitutive activation of downstream signal transduction pathways in *suppressor of npr1-1, constitutive 1*. *Plant Cell* 15: 2636–2646.

Zhang Y, Shi J, Liu J-Y, Zhang Y, Zhang J-D, Guo X-Q. 2010. Identification of a novel NPR1-like gene from *Nicotiana glutinosa* and its role in resistance to fungal, bacterial and viral pathogens. *Plant Biology* 12: 23–34.

Zhou J, Zhang Y. 2020. Plant immunity: danger perception and signaling. *Cell* 181: 978–989.

Supporting Information

Additional Supporting Information may be found online in the Supporting Information section at the end of the article.

Fig. S1 The exon-intron organization in the BTB/POZ-encoding regions are highly conserved between NPR and BOP families.

Fig. S2 Gene duplications in Brassicaceae-specific NPR subclades and integration of *Boechera stricta* NPR1 homolog into TIR-NLR protein, related to Fig. 1(a).

Fig. S3 Phylogenetic tree showing the conservations of functional residues and motifs of 194 NPR proteins, related to Fig. 1.

Fig. S4 Generation of Mp*npr* mutants using CRISPR/Cas9 system and complementation of the SA-hypersensitivity phenotype in the mutants.

Fig. S5 BTH sensitivity was unchanged in Mp*npr* mutants compared to Tak-1.

Fig. S6 RNA-Seq analysis comparing Tak-1 and Mp*npr-1^{ge}* thalli in mock and SA conditions.

Fig. S7 RNA-Seq analysis comparing Tak-1 and Mp*npr-1^{ge}* gemmae in SA and BTH conditions.

Fig. S8 Enhanced thermomorphogenesis in Mp*npr* mutants.

Fig. S9 Quantitative data of Mp*npr-1^{ge}* expressing Mp*NPR^{R413Q}* and recombinant NPR proteins used in MST.

Table S1 Oligonucleotides used in this study.

Table S2 NPR and BOP homologs used for phylogenetic analysis.

Table S3 Reference genomes of species used in BLASTP.

Please note: Wiley is not responsible for the content or functionality of any Supporting Information supplied by the authors. Any queries (other than missing material) should be directed to the *New Phytologist* Central Office.